Interhemispheric differences in cirrus properties from anthropogenic emissions

INCA

Annual Report 2

PERIOD COVERED BY THE REPORT: MONTH 13-24

CONTRACT Nº: EVK2-1999-00039

PROJECT COORDINATOR: DR. JOHAN STRÖM
STOCKHOLM UNIVERSITY

CONTRACTORS:

1.	Stockholm University	S
2.	Deutsches Zentrum für Luft- und Raumfahrt	D
3.	University Blaise Pascal	F
4.	Centre National de la Recherche Scientifique	F
5.	University of Helsinki	FIN
6.	Norsk institutt for luftforskning	NO

PROJECT HOMEPAGE: http://www.pa.op.dlr.de/inca/

CONTENT:

1. Executive publishable summary, related to reporting period

Contract n°	EVK2-1999-00039	Reporting period:	Months 13-24
Title	Interhemispheric differences in cirrus properties from anthropogenic emissions		

Objectives:

The INCA project has two overall objectives and these are:

1) **Determine the difference in cirrus properties, which are of importance for climate and ozone distribution in the upper troposphere and lower stratosphere, in air masses with low and high aerosol loading.**

2) **Provide the fist set of data of the microphysical and morphological properties of young cirrus clouds at southern and northern mid-latitude, in relatively clean and polluted air masses, under otherwise comparable conditions.**

The objectives of the second reporting period were to prepare the data from the two measurement campaigns performed during the first reporting period. The data has been checked and uploaded to the database, which is available through the INCA web page. Because no field activities were planed for the second period, analysis and interpretation of the data was the main focus of the second reporting period.

Scientific achievements:

The INCA project has provided the first set of data of aerosol and cirrus cloud properties in the southern hemisphere mid-latitudes. By performing a second observation campaign in the northern hemisphere, at equal latitudes, at equivalent season, using the same equipment and conducting both campaigns within one year, the INCA project has also provided a unique set of data that allow for a direct comparison of pristine and polluted environments. The observations cover important trace gases such as CO, O_3, NOx, NOy and H_2O; size distributions; elemental composition and thermal stability of ambient aerosols and crystal residual particles; michrophysical and optical properties of cirrus crystals as well as atmospheric state and three dimensional wind.

Socio-economic relevance and policy implications:

Scientific assessments are used by policy makers to base long-term decisions that affect a large number of people. In recent assessments dealing with the atmosphere and the climate system it is repeatedly emphasized that critical understanding about the aerosol-cloud-climate interaction is missing. The contribution of new understanding provided by INCA in an area poorly understood will undoubtedly have an important part in future assessments on the human impact up on the atmosphere.

Conclusions:

Conclusions drawn from the analysis of INCA data are many in details, but can be summarised in two major topics.

1) We can conclude that the levels of pollution in the tropopause region of the Southern- and Northern hemisphere mid-latitudes are distinctly different. The Northern hemisphere shows several times higher loading of trace gases and aerosols.

2) We can conclude that a difference in cloud related properties are evident in the data. The relative humidity associated with cirrus clouds is higher in the Southern Hemisphere. The fraction of non-volatile particles found in crystals is higher in the Southern Hemisphere. The ice crystals are fewer and larger in the Southern Hemisphere.

The sensitivity of the system in the sense of a quantitative relation between an anthropogenic perturbation and a response in the cloud properties require more in-depth analysis of the data, since in-situ observations simply provide a statistical sample of the atmosphere.

Keywords:

Cirrus, aerosols, aircraft, emissions, contrails, ozone, climate, tropopause

Publications (cumulative list)[1]

General rules about publicity and communications are defined within the Annex II ,"General conditions" Part B, to the contract, mainly obligations, responsibilities and reference to Community support. This should be prepared as a separate page to be annexed to the report and updated annually.

Peer Reviewed Articles:

Authors	Date	Title	Journal	Reference
Ovarlez, J., Auriol, F., Brissot, J.-B., Busen, R., Gayet, J.-F., Gierens, K., Ovarlez, H., Schumann, U., Ström, J	2002	Water Vapour Measurements Inside Cirrus Clounds in Northern and Southern hemispheres during INCA.	Geophys. Res. Lett.,	Submitted.
Gonzalez A., P. Wendling, B. Mayer, J-F Gayet and T. Rother	2002	Remote sensing of multilayer cirrus cloud properties during INCA using ATSR-2 data: Case study on 23 March	J. Geophys. Res..	Submitted
Gayet J-F, F. Auriol, A. Minikin, J. Strom, M. Seifert, R. Krejci, A. Petzold, G. Febvre and U. Schumann	2002	Quantitative measurements of the microphysical and optical properties of cirrus clouds with four different in situ probes: Evidence of small ice crystals.	Geophysical Research Letters	Submitted
Gierens K., M. Monier and J-F Gayet	2002	The deposition coefficient and its role for cirrus clouds.	Journal of Geophysical Research	Submitted

Non refereed literature:

Authors / Editors	Date	Title	Event	Reference	Type[2]
Ström, J., U. Schumann, J.-F. Gayet, J. Ovarlez, F. Flatoy, M. Kulmala, O. Schrems, P. Minnis, S.B. Diaz, B. Milicic, V. Valderama, E. Amthauer, J. Pettersson, and F. Arnold	2000	Aerosol and Cirrus Measurements at Midlatitudes on the Southern Hemisphere- An overview based on the first INCA Experiment	Aviation, Aerosols, Contrails andCirrus Clouds (A2C3), European Workshop, Seeheim	Seeheim (nearFrankfurt/Main), Germany, July 10-12	Proceeding
Ovarlez, J., H. Schlager, P. van Velthoven, E. Jensen, U. Schumann, H. Ovartlez, and J. Ström	2000	Water vapour measurements in the upper troposphere from POLINAT and other campaigns	Aviation, Aerosols, Contrails andCirrus Clouds (A2C3), European Workshop, Seeheim	Seeheim (nearFrankfurt/Main), Germany, July 10-12	Proceeding
Strom J., F. Flatoy, J.-F. Gayet, M. Kulmala, J. Ovarlez and U. Schumann,	2000	Observations in cirrus clouds during the INCA Southern Hemisphere campaign	*13th Int. Conference on Clouds and*	Reno, USA, 14-18 August 2000	Proceeding

[1] Two copies of publications issued during reporting period should be annexed to the report, specific cases should be agreed by the Project Officer

[2] Type: Abstract, Newsletter, Oral Presentation, Paper, Poster, Proceedings, Report, Thesis

			Precipitation.		
Andreas Minikin, Andreas Petzold, Johan Ström, Radek Krejci, Marco Seifert, Helmut Ziereis, Hans Schlager, Reinhold Busen, Ulrich Schumann:	*2001*	*Interhemispheric differences in the fine particle load of the upper troposphere.*	*EGS 2001, Nice, 25-30 March*		Oral presentation
A. Minikin, A. Petzold, J. Ström, R. Krejci, M. Seifert, J. Baehr, H. Ziereis, H. Schlager, R. Busen, U. Schumann :	2001	Properties of the upper tropospheric background aerosol in the southern hemisphere	IAMAS, Innsbruck, 10-18 July		Oral presentation
A. Minikin, A. Petzold, J. Ström, R. Krejci, M. Seifert, J. Baehr, H. Ziereis, H. Schlager, R. Busen and U. Schumann:	2001	Interhemispheric differences in the properties of the upper tropospheric background aerosol.	European Aerosol Conference Leipzig, 2-7 Sept	Journal of Aerosol Science, Vol. 32, Supplement 1, S1043-S1044, 2001	Oral presentation
Auriol F., J.F. Gayet, J. Ström and A. Petzold,	2001	On microphysical & optical properties of cirrus clouds in Southern and Northern hemispheres.	*XXVI General Assembly*, *European Geophysical Society*	Nice, France, 25-30 March 2001	Proceeding
Seifert M., J. Ström, R. Krejci, A. Petzold, A. Minikin, J.F. Gayet, F. Auriol, U. Schumann, R. Busen	2001	In situ observations of aerosols particles remaining from evaporated cirrus crystals :a comparison between clean and polluted conditions	*XXVI General Assembly*, *European Geophysical Society*	Nice, France, 25-30 March 2001	Proceeding
Ziereis H., J. Baehr, A. Petzold, A. Minikin, P. Stock, H. Schlager , J.-F. Gayet, J. Ström, R. Busen,U. Schumann	2001	In situ observations of Noy uptake by cirrus clouds during INCA	*XXVI General Assembly*, *European Geophysical Society*	Nice,France, 25-30 March 2001	Proceeding
Ovarlez, J., J.B. Brissot, H. Ovarlez, F. Auriol, J.F. Gayet, R. Busen, A. Minikin, A. Petzold, U. Schumann, and J. Ström	2001	Some observations on the water vapor saturation level inside and around cirrus clouds during the INCA campaigns.	GEWEX Meeting	Paris, 10-14 September	Oral presetation
J. Ovarlez[1], H. Ovarlez[1], F. Auriol[2], J. F. Gayet[2], R. Busen[3], A. Minikinn[3], A. Petzolt[3], U. Schumann[3] and J. Ström[4]	2001	Some observations on the difference of cirrus clouds water vapor saturation level in polluted and not polluted area during the INCA campaign.	*8th Scientific Assembly of IAMAS*	Innsbruck, Austria, 10-18 July 2001	Proceeding
Baehr, J., H. Ziereis, P. Stock, H. Schlager, R. Busen, J. Ström and U. Schumann	2001	Reactive nitrogen observations in the upper troposphere of the northern and southern hemisphere during INCA	*XXVI General Assembly*, *European Geophysical Society*	Nice,France, 25-30 March 2001	Proceeding
Gayet, J-F, F. Immler, F. Auriol, A. Minikin, J. Ovarlez and J. Ström.	2002	Microphysical and optical properties of a cirro – cumuls sampled during the INCA experiment.	AMS Cloud Physics conference, Ogden (USA) June 2002		Oral Presentation
Andreas Minikin, Andreas Petzold, Markus Fiebig, Johan Ström, Radek Krejci, Marco Seifert, Peter van	2002	Intercomparison of background aerosol properties of the mid-latitude upper troposphere in the	EGS 2002, Nice, 22-26 April		Poster

Velthofen, Janine Baehr, Helmut Ziereis, Hans Schlager, Reinhold Busen, Ulrich Schumann:		northern and southern hemisphere.			
Immler F., O. Schrems, J-F Gayet, F. Auriol, A. Minikin, A. Petzold and J.Ström	2002	Ground-based lidar measurements of cirrus clouds in the Northern and Southern hemisphere (INCA) comparison with in situ measurements.	XXVII General Assembly, European Geophysical Society, Nice,		Oral
Gonzalez A., P. Wendling, B. Mayer, J-F Gayet and T. Rother	2002	Remote sensing of multilayer cirrus cloud properties during INCA using ATSR-2 data: Case study on 23 March	11th AMS conference on Cloud Physics, 3-7 June 2002, Ogden, Utah		Oral

Others: (Patents, CD ROM's, videos,…)

Planning of future publications: (type, date, contents, …)

Minikin et al., Interhemispheric differences in the fine particle load of the upper troposphere.			Geophys. Res. Lett.	To be submitted
Minikin et al., Chemical properties of the free-tropospheric aerosol: A comparison between the polluted NH and the clean SH.				
Gayet J-F, F. Auriol, J. Ovarlez, A. Minikin, K. Gierens, J. Ström and U. Schumann	2002	Interhemispheric differences in microphysical and optical properties of cirrus clouds sampled during the INCA experiment.	Journal of Geophysical Research	Article
Gayet J-F, F. Auriol, J. Ovarlez, A. Minikin, J. Strom and U. Schumann	2003	An overview of microphysical and optical properties of cirrus clouds observed in the Southern hemisphere during INCA	Journal of Atmospheric Sciences	Article

2. Objectives

The overall INCA objectives are:

2) **Determine the difference in cirrus properties, which are of importance for climate and ozone distribution in the upper troposphere and lower stratosphere, in air masses with low and high aerosol loading.**

2) **Provide the fist set of data of the microphysical and morphological properties of young cirrus clouds at southern and northern mid-latitude, in relatively clean and polluted air masses, under otherwise comparable conditions.**

The objectives of the second reporting period were to prepare the data from the two measurement campaigns performed during the first reporting period. The data has been checked and uploaded to the database, which is available through the INCA web page. Because no field activities were planed for the second period, analysis and interpretation of the data was the main focus of the second reporting period.

The wealth of data gathered during the INCA project is by no means fully exploited within the one year available and the work of interpret the data has really only begun. Some of the first results available up to the end of the contract are presented in this report as well as in the final report of the project.

The second reporting period also included the aim to present INCA data at various conferences to quickly reach out with our findings and get feedback from peers in the field. This was done very successfully and many contacts where taken, and the interest in using INCA data by other scientists outside the INCA team is very large.

As a primer for the analysis work with INCA data a list of scientific goals where made. All of these questions are not answered on the short duration of INCA, but the material is now available to address these issues and in many cases make definite breakthroughs.

LIST of scientific questions

- Is the onset of cirrus different in clean vs. polluted air masses?
- Is the lifetime of cirrus clouds (e.g. evaporation rates) different in a clean vs. a polluted air mass?
- What is the phase of young cirrus clouds? Is the phase dependent on where cirrus clouds form?
- On what type of nuclei do cirrus clouds form?
- Can we define clear differences in nuclei in air over continents vs. air over oceanic regions?
- What are the cloud nucleating properties of ambient aerosol particles and particles in air affected by aircraft exhaust?
- Can we find evidence for aircraft exhaust particles in thin cirrus clouds ice particles, and in what proportions?

- Can the mass loading of carboneous aerosols be related to changes in cirrus clouds affected by aircraft exhaust?
- Can knowledge of aerosol particle properties and dynamics of air motions be related, by way of known nucleation processes, to the concentration and distribution of ice particles formed in clouds?
- How do clouds modify the properties of aerosol, or scavenge them?
- What is the effect of cloud processing of aerosol size distribution and CCN and IN activity?
- Do cirrus influence ozone production and loss? Is it possible to distinguish an ozone gradient in cirrus dependent on microphysical properties?
- Which of the thermal tropopause or the hygropause are more appropriate to determine the vertical extent of cirrus?

3.1 WP1: Project coordination

Start date: 0
End date: 24
Lead contractor: 1

Project coordination during the first reporting period involved more interaction between the partners that often needed immediate reactions or responses form partners in order to perform the two field campaigns in time, make best use of the flight hours and assure the highest quality in the data.

After the campaigns each partner worked on the data to get it at a level that could be uploaded to the database. A project meeting was held in March 2001, with the purpose to survey the status of the data and plan the remainder of the project. The wealth of data took more time than anticipated to prepare in a condition (quality assured) to be put on the database. This has caused a delay in the publication of results in peer-reviewed journals, but not a shortage in ideas and potential topics for publications. To the contrary, the in-depth work with the data have emphasised the strength in the analysis when combining observations from different sensors. This has already been proven in some of the already submitted manuscript. Hence, much conversations and discussions about the data and how to proceed with the analysis work has been conducted between meetings via electronic mail.

A second and final INCA meeting was held towards the end of 2001. As in previous meetings associated partners were also invited to participate. Extremely valuable contributions from in particular NASA, KNMI, and AWI have really given the INCA-project extra value. Remote sensing products from satellite and Lidar data together with model products such as trajectory calculations allows to put the in-situ observations into a three dimensional context.

In summary, the project essentially developed as anticipated and no really serious delay was encountered. The campaigns were conducted as scheduled and the database was complete at the end of the project. Extremely, high data efficiency was achieved with a very small fraction of data lost due to instrument problems. Thanks to internal funding more flight hours could be generated, which allowed for measurements being conducted during ferry flights. These data are also available through the INCA web page as is contributions from some associated partners.

Some of the costs associated with the two campaigns took some more time to balance than anticipated. The reason for this was the intention to save funds for the project through coordinating the expenses in the field. The drawback is that all these details need to be organized after the campaigns. Some of the bills had to be returned to Chile because of some erroneous items. However, these things are now resolved.

The final task of project coordination is the work of synthesizing individual contributions from the partners into the numerous reports associated with projects of this type.

3.2 WP2: Campaign support

Start date: 0
End date: 12
Lead contractor: 6

The second year of INCA included no field activities since it was part of the strategy to complete the two measurement campaigns within the same year of the first reporting period. The reason for this was partly due to technical considerations and partly for scientific reasons. A short time between campaigns helps keeping the integrity of the instruments, which would otherwise risk having to go through major overhaul and adjustments. The other reason is to be able to compare equivalent seasons for the two campaigns. Finally, a long period between campaigns also runs a larger risk that a major volcanic event or a phenomenon such as El Nino significantly change the ambient conditions between campaigns.

Hence, the second reporting period include no specific campaign support, but the work with the database may be viewed as the final part of this task. This work also link to project coordination in that a significant contribution to the database has been provided through collaboration with associated partners to INCA.

The support by NASA (the group of Dr. Pat Minis) in providing satellite products with flight track overlays etc. is very helpful when interpreting the in-situ data. The support by KNMI (Dr. Peter van Velthoven) in providing trajectory calculations and products extracted from the ECMWF model, give the possibility to put the in-situ measurements in context of the three dimensional atmosphere. The INCA team was very fortunate to also have the Lidar MARL from Alfred Wegener Institute (group of Prof. Otto Schrems) present during both field campaigns. Statistics from this instrument gives valuable information about how representative the data sampled during the campaign is, and the possibility to compare remote and in-situ sampling inside cirrus clouds. The fields from the NILU-CTM model used during the campaign planning are also accessible via the INCA home page. Post campaign access to these data also gives excellent means to link in-situ observations with the three dimensional atmosphere. In addition there are other auxiliary information, such as air traffic density, available through the INCA web page http://www.pa.op.dlr.de/inca/ .

The work of managing the database is performed by DLR and accessed through the INCA home page. Currently the database is protected by means of password to be able to track by whom and how data is being used.

3.3 WP3: Cloud microphysical properties

Start date: 0
End date: 24
Lead contractor: 3

INCA data permit the determination of cloud element number and bulk densities by various independent techniques : CVI (operated by partner 1), FSSP-300 (partner 2), 2D-C and Polar Nephelometer (partner 3). The combination of these four techniques provides a full description of particles within a diameter range from a few micrometer (typically 3 μm) to 800 μm. Because of the presence of small ice crystals in cirrus clouds, it was particularly important to overcome the limited accuracy of the sensors used in the experiments for cloud microphysical measurements. This has been the first step within the strategy of data processing and interpretation.

The reliability of the microphysical cirrus measurements by the different probes listed above was assessed from systematic probe comparisons and the results were discussed in a paper submitted to *Geophysical Research Letters* (Gayet et al., 2002). Following the recommendations of the reviewers and because the small ice particles are not spherical (a typical asymmetry parameter of 0.77 was measured during INCA with the Polar Nephelometer) the FSSP-300 size calibration for aspherical particles has been considered. Therefore the upper size limit of the FSSP-300 for cirrus measurements is actually 15.8 μm compared to 20 μm nominally used. The PMS 2D-C probe data have also been re-evaluated in order to take into account the sensitivity of the probe to small particles that decrease with the airspeed (i.e. ~ 170 m/s with the Falcon aircraft). Therefore, the six-first channels (up to 150 μm) have been corrected.

The new results show a reasonable agreement between the two size distributions measured by the FSSP-300 and the 2D-C probes by considering the updated FSSP-300 size calibration and the airspeed corrections on the first 2D-C channels. This feature together with the results of the comparisons between the calculated bulk quantities (particle surface and volume) based on the PMS size distributions and those derived from independent absolute measurements (Polar Nephelometer and Lyman-α) give robust proof of the reliability of both the measurements of small ice particles by the FSSP-300 and our method of data processing.

As a conclusion we can say that a systematic comparison between four independent techniques for the measurement of cirrus microphysical and optical properties confirms the reliability of the measurements and provides a robust foundation for the interpretation of the observations from the Southern and Northern hemisphere experiments.

Proofs and quantitative values have been obtained concerning the number and bulk densities of small ice crystals in cirrus clouds. Despite inherent shortcomings of the probes, the methods of data processing and additional uncertainties due to a possible ice crystal shattering, similar orders of magnitude on microphysical parameters have been derived from four independent techniques. Numerous small particles are present in cirrus even in moderate vertical velocities of typically ± 0.3 m s^{-1}.

These observations presented above have implications for the modeling of the formation and evolution of cirrus clouds since models simulating the INCA cases should arrive to a similar crystal number density. This was the second step within the strategy of the interpretation of INCA data. In this way, Gierens et al. (2002) suggested that the potential of homogeneous freezing to produce large number of ice

crystals in region of gentle aircraft has been underestimated so far. Small but realistic deposition coefficients for small ice crystals lead to longer periods with relative humidity near the critical value for nucleation, which results in much larger numbers of ice crystals than with deposition coefficients close to unity. This mechanism allows reproducing number densities of ice crystals in the 10 - 30 μm size range obtained from the INCA measurements. This was investigated by varying the deposition coefficient in numerical simulations of homogeneous cirrus formation using a parcel model with spectrally resolving microphysics. Subsequently, three microphysical parameters have been considered: the growth of sulphuric acid solution droplets, their homogeneous freezing and the depositional growth of the resulting ice crystals.

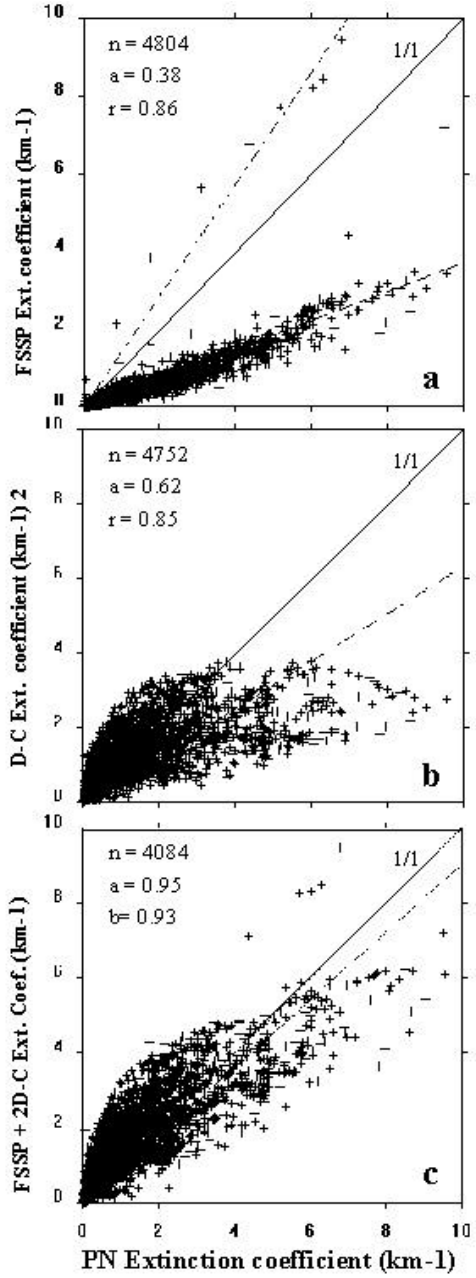

Figure 3.3.1. Extinction coefficient measured by the Polar Nephelometer versus the extinction coefficient inferred from: (a) the PMS FSSP-300, (b) the PMS 2D-C and (c) the PMS FSSP-300and 2D-C probes. The symbols n, a and r refer to the number of data points, the slope of the best-fit curve equation (dashed lines) and the correlation coefficient respectively

The next step within the strategy of the INCA project was to proceed to the analysis of the results and to the comparison of the pertinent cirrus microphysical and optical parameters between the two hemispheres. The data set used in this study includes the 1-Hz measurements performed during 11 flights carried out in the Southern hemisphere and 10 flights in the Northern hemisphere. During the two campaigns several different types of cirrus have been sampled including: cirrostratus, jetstream-cirrus, cold and warm frontal cirrus, cirrocumulus orographic-wave cirrus, anvil-cirrus. For additional information on the INCA project and flight logs we refer to: http://www.pa.op.dlr.de/inca/.

Only cirrus-clouds observed at temperature lower than –35°C have been considered. The in-cloud criterion has been defined using the extinction coefficient from the Polar Nephelometer with values larger than a threshold of 0.2 km^{-1}, which roughly corresponds to a concentration of ice particles of 0.2 cm^{-3} with a diameter of 5 μm. Hence, the analysis does not include the thin cirrus clouds that were mainly observed in the Northern Hemisphere (Result from WP 5 and Franz Immler personal communication).

The frequency distribution of the in-cloud temperature for the two campaigns show very similar temperature feature for both the two data sets with a mode near –45°C and extended down to –60°C and –63°C for the SH and NH experiments, respectively. As a consequence, bias on the comparison results due to different thermodynamical conditions is considerably reduced. Nevertheless, it should be noticed that the number of data points are larger for the SH experiment (28229) than for the NH campaign (17359).

Most of the results which concern the parameters comparison between the two hemispheres has been discussed as a function of the relative humidity with respect to ice (*RHi*). The representative statistical parameters used in our analysis are the median values and the 25 and 75 percentiles. These parameters have been considered instead of the mean value and the standard deviation because of the non-Gaussian frequency distribution of each considered parameters. Statistical significance levels of the results are satisfied (< 1%) for *RHi* values larger than 85% and lower than about 130%. For *RHi* < 85% and *RHi* > 130% the number of data points are insufficient with rather large dispersion of the parameter values.

The parameters analysis and the comparison results between the two hemispheres has been proceeded for the following parameters: Ice particle concentration, Ice water content, Extinction coefficient, Effective diameter, Mean diameter of large ice crystals (D> 50 μm) and Asymmetry parameter. The results has been thoroughly presented and discussed in Gayet et al. (2002). They can be summarized as the following:

Within the range of relative humidity (with respect to ice) between 85% and 130% the results presented above are statistically significant. These results clearly evidence systematic and significant differences in microphysical and optical properties of the cirrus clouds sampled during the Punta Arenas and Prestwick campaigns. Obviously, these differences cannot be generalized to the Northern and Southern hemispheres cirrus properties as a whole. Nevertheless, compared to the properties of cirrus clouds in the Punta Arenas area, the cirrus sampled from Prestwick are characterized by a larger concentration (ratio of about 2) of ice crystals, which have a lower effective diameter (about 20%, see Figure 3.3.2). These size differences are more pronounced for large ice crystals (i.e. > 50 μm) and are confirmed by the differences in the asymmetry factor that is measured by an independent technique. Our results are in qualitative agreement with the

observations of Ström and Ohlsson (1998) who observed enhanced crystal number densities in regions where the cloud particles contained elevated levels of absorbing material taken as a proxy for anthropogenic influence. Kristensson et al. (2000) showed that this influence caused a reduction of the effective diameter by 10-30% in the polluted cirrus.

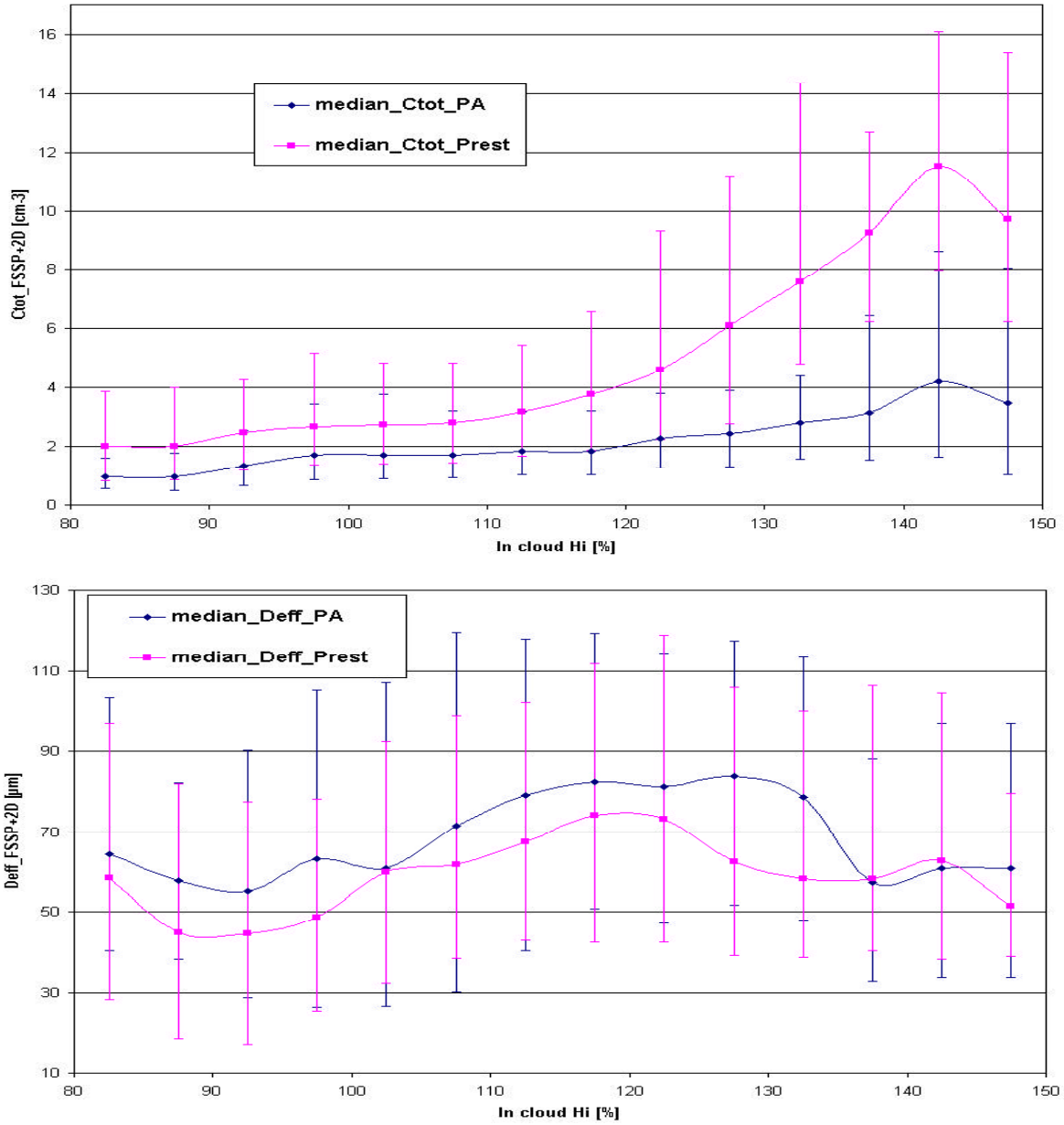

Figure 3.3.2 : Ice particle concentration (upper figure) and effective diameter (lower figure) versus the relative humidity with respect to ice for the cirrus clouds sampled in the southern and northern hemispheres. The full circle symbols are the median values and the vertical bars represent the 25% and 75% percentiles interval. The thick lines are interpolations of the median values.

3.4 WP4: Aerosol properties

Start date: 0
End date: 24
Lead contractor: 2

The interstitial/out-of-cloud aerosol instrument package operated onboard the DLR Falcon was described in detail in the first year report. The instrumentation included several condensation particle counters (CPCs) with unheated and heated inlets, optical particle counters (OPC, PCASP), a differential mobility particle sizer (DMPS), and an aerosol absorption photometer (PSAP). In addition, aerosol samples were taken for single-particle chemical (elemental) analysis of aerosol particles. The combination of the instruments allowed to determine size resolved number concentrations of aerosol particles over the whole relevant size range of upper tropospheric background aerosol, that is from ultrafine particles (smallest detectable particle diameter 3 nm) to accumulation mode and coarse mode particles (100 nm up to about 1 μm).

The post-campaign processing of the aerosol measurements taken during the second INCA campaign in Prestwick was part of the second year of the project and has been completed. For both campaigns, the rather time-consuming processing of DMPS and absorption data has been completed during the second year as well. All data have been added in a standard data exchange format to the INCA data archive, which is accessible through the internet <http:\\www.pa.op.dlr.de\inca\data>. A detailed overview of the instruments status and data availability of each flight can be found at <http://www.pa.op.dlr.de/inca/data/INCAda-InstrumentStatus.html>.

The chemical analysis of the aerosol filter samples was completed in collaboration with the Technical University of Munich, Institute of Hydrochemistry (Dr. Ulrich Poeschl). Since the analysis of single particles by SEM/EDX (scanning electron microscope with an energy-dispersive X-ray detector) is very time-consuming, results of the analysis were available only late during the second project year and have not yet been investigated in detail. Minimum particle diameters suitable for elemental analysis were about 200 nm. Smaller particles down to 50-100 nm are visible on the images taken by the SEM. Most samples show the presence of alkali metals and other elements typically found in crustal material. It is currently being investigated if quantification of C and O peaks in the spectrum is possible to derive information about organic content.

For the detailed analysis of the aerosol data from the SH and the NH campaigns and from the transfer flights to and from Punta Arenas, extensive use has been made of data from other work packages: Ozone and carbon monoxide from WP 6 were used as air mass tracers for stratospheric and anthropogenically influenced boundary layer air, respectively. To distinguish between in-cloud and out-of-cloud situations cloud physical data of WP 3 were used. Atmospheric state data (WP 7) as well as forecast/analysis data of the meteorological situation (WP 2) were needed to derive information for example to relate the Falcon flight track to the actual meteorological situation and tropopause position.

The vertical aerosol profiles show significant features in the upper troposphere (UT), which makes it necessary to account for tropopause (TP) heights when comparing data or deriving averaged profiles. TP heights were identified from the Falcon measurements (ozone, temperature profiles) or, if the Falcon did not penetrate the lower stratosphere, from ECMWF analysis data (potential vorticity data). At the SH campaign TP heights varied between 8500 and 12000 m, at the NH

campaign between 8000 and 12500 m, with a typical and average value of 10500 m, which is representative for both campaigns. Some results of the statistical analysis of integral aerosol properties like number concentration of Aitken particles (condensation particles with diameters larger than 14 nm), of accumulation mode particles (particles between 100 nm and 1 μm diameter), and of non-volatile particles (remaining condensation particles larger than 10 nm after treatment with 250°C heating) are presented in condensed form in Table 3,4,1 and Figure 3.4.1. This analysis is based on carefully selected and validated subsets of data which are believed to be reasonably representative for the SH and NH mid-latitude upper troposphere within the natural limitations imposed by the given observation periods of 3-4 weeks and the probing with 10-12 flights at each campaign. The comparison of NH and SH concentration levels in the different vertical regimes of the troposphere cannot be explained in detail here. The main feature emerging consistently is that aerosol number concentrations in the NH are higher (on average a factor of 2-3) than in the SH and much more variable (see Table 3.4.1 and Figure 3.4.1). The case of 12-Oct-2000 during the Prestwick campaign is a remarkable example for this variability in the sense that at that day extremely high pollution was observed along with strong particle nucleation apparently as a result of strong convection going on even over ocean areas.

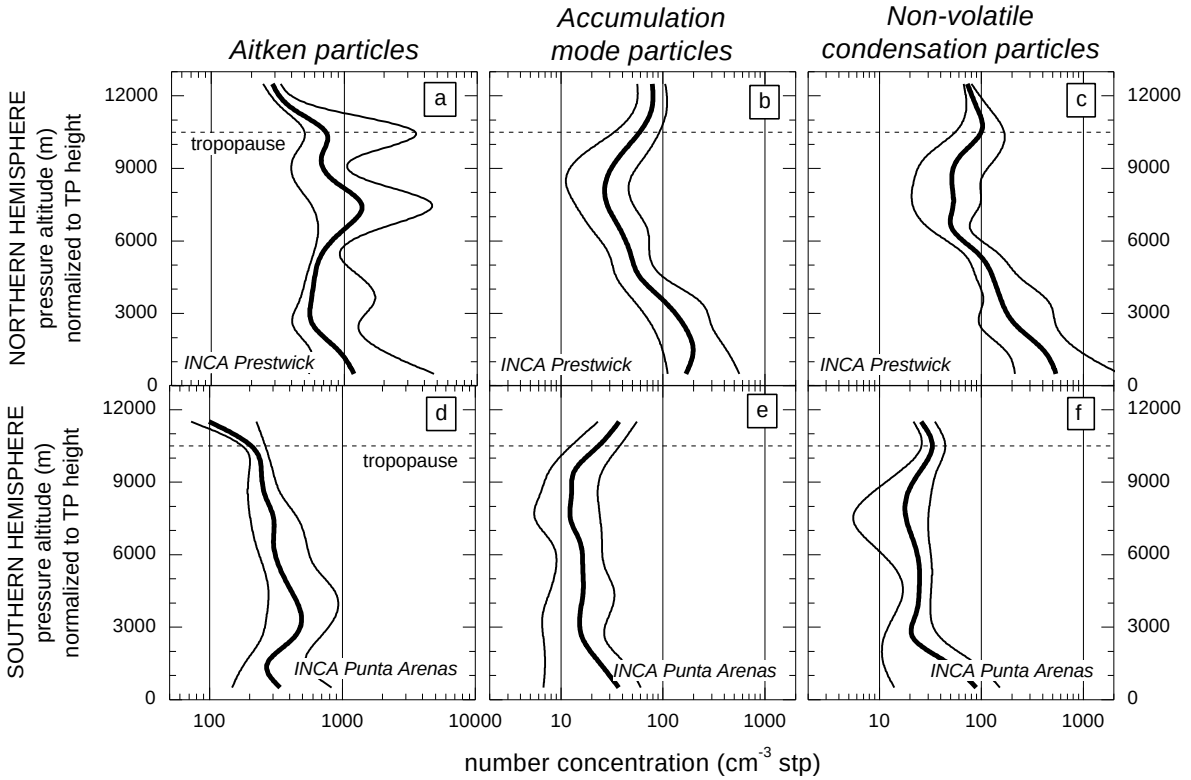

Figure 3.4.1: Mean vertical profiles of aerosol number concentrations (Aitken, accumulation mode and non-volatile aerosol particles) for the INCA Prestwick (a-c) and the INCA Punta Arenas (d-f) campaigns. To facilitate the comparison of each flight's data, the pressure altitude scale of each flight was normalized in order to match the actual tropopause (TP) heights to the mean TP height of 10500 m (valid for both INCA campaigns). Number concentrations have been calculated to represent standard conditions. The thick lines refer to the median, the thin lines to the 25- and 75-percentiles of the data binned into 500 m altitude intervals.

As for the aerosol volatility measurements made during INCA (semi-volatile and non-volatile aerosol fractions) it will be possible to give more profound interpretation of the results in the very near future. In on-going laboratory investigations the

thermodenuder/condensation particle counter systems used onboard the Falcon are being characterized in detail with respect to particle losses and efficiency of the heat treatment. As a preliminary result it can be stated that the relative fraction of non-volatile (refractory) particles in the UT is about 10 % and apparently somewhat higher in the SH if compared to the NH. In the NH roughly 50 % of the non-volatile particles, in the SH slightly more, consist of larger particles in the accumulation mode size range (larger than 120 nm).

The absorption measurements of the background aerosol made during INCA in particular in the middle and upper troposphere were affected by instrument limitations with the aerosol absorption being predominantly below detection limit. The average absorption coefficient is below 1-2 x $10^{-6}m^{-1}$ throughout the troposphere in the SH, whereas the absorption coefficient in the NH is on average much higher in the boundary layer (6-8 x $10^{-6}m^{-1}$) and steadily decreasing towards the UT. UT differences between both hemispheres could not be determined because the absorption coefficients here fall always below detection limit.

The analysis of the data from the transfer flights from Europe to Southern Chile and back has shown that the background aerosol concentration in the upper troposphere is significantly different in the mid-latitudinal regions of the NH and SH with the SH being cleaner. Aerosol concentrations in the tropical regions clearly exceed the background values in the mid-latitude regions, even those of the NH, which is mainly due to different aerosol sources and the very strong convection processes going on in the tropics.

Aerosol components in the SH show relatively weak vertical gradients indicating that the troposphere of the SH is relatively well mixed, that is, surface sources are of minor importance, and that aerosol on average will be relatively aged due to long transport times. The situation in the NH is much more complex due to a greater variety of air masses with different source regions that carry different levels of pollutants. In particular the accumulation mode and the non-volatile aerosol (the latter partly constituting the accumulation mode aerosol particles) show in the NH a pronounced and steady decrease from the surface towards the upper troposphere. However, in spite of this strong vertical gradient the aerosol concentrations even in the tropopause region remain higher than that observed in the SH. Why the accumulation mode and non-volatile aerosol is slightly enhanced just above the tropopause (in both hemispheres) is not yet explained. (One has to take into account that data of the TP region are less representative, because the Falcon did not fly this high very often during INCA.) The overall vertical gradients observed in the NH indicate the large-scale importance of anthropogenic and, to a minor degree, natural surface sources for the NH middle and upper tropospheric aerosol budget. It is clear from these observations that the abundance and most likely also the chemical properties of the aerosol taking part in cirrus cloud formation will be systematically different between both hemispheres. Indeed, systematical differences in cirrus properties between both hemispheres have been found during INCA (see other WPs).

The aerosol measurements of INCA do compare quite well with observations from other aircraft campaigns as far as these are comparable. They do not agree with the very few published model results on the global scale distribution of fine aerosol showing that global models are not yet able to accurately predict upper tropospheric aerosol properties and in particular large scale variations thereof. The INCA aerosol data set will certainly prove to be very important to further verify and test the ability of actual and forthcoming global aerosol models.

Table 3.4.1: Intercomparison of aerosol number concentrations between northern hemisphere (NH) and southern hemisphere (SH) for the mid-latitude upper troposphere (UT), middle troposphere (MT) and lower stratosphere. For the UT and MT values without parentheses refer to cloud-free flight conditions, values in parentheses refer to all data including cloud passages. The range is defined by the 10- and 90-percentiles. Data have been selected for time periods where the tropopause (TP) is well defined and shows essentially no vertical gradient (approx. 10 % of data excluded).

Upper Troposphere (from 2000 m below TP to approximate TP height)							
	SH (INCA Punta Arenas)			*NH (INCA Prestwick)*			
	number concentration (1/cm³ stp)		observation time (s), number of flights	number concentration (1/cm³ stp)		observation time (s), number of flights	NH/SH factor
	median	range		median	range		
Aitken particles (d_p > 14 nm)	320 (306)	151...601 (172...667)		950 (682)	380...17100 (172...12800)		3.0 (2.2)
ultrafine particles (5 nm > d_p > 14 nm)	99 (110)	47... 743 (53...836)	3536 (9889),	750 (372)	75...7260 (232...18100)	2061 (6157),	7.6 (3.4)
accumulation mode part. (d_p > 120 nm)	21 (20)	8...42 (8...47)	12 (12)	48 (47)	20...109 (18...106)	11 (12)	2.3 (2.3)
non-volatile particles (d_p > 10 nm)	37 (29)	11...74 (11...65)		100 (85)	24...811 (17...502)		2.7 (2.9)
Middle Troposphere (from 6000 m altitude to 2000 m below TP)							
	SH (Punta Arenas)			*NH (Prestwick)*			
	number concentration (1/cm³ stp)		observation time (s), number of flights	number concentration (1/cm³ stp)		observation time (s), number of flights	NH/SH factor
	median	range		median	range		
Aitken particles (d_p > 14 nm)	286 (352)	145...558 (163...906)		964 (798)	265...13700 (170...3670)		3.3 (2.3)
ultrafine particles (5 nm > d_p > 14 nm)	89 (177)	28...471 (34...941)	2634 (7456),	658 (424)	66...5900 (41...4020)	3705 (6656),	7.4 (2.4)
accumulation mode part. (d_p > 120 nm)	15 (20)	4...35 (6...63)	11 (12)	35 (36)	14...89 (10...136)	10 (11)	2.3 (1.8)
non-volatile particles (d_p > 10 nm)	28 (17)	5...61 (5...54)		58 (50)	16...167 (9...151)		2.1 (2.9)
Lower Stratosphere (ozone > 200 ppb)							
	SH (Punta Arenas)			*NH (Prestwick)*			
	number concentration (1/cm³ stp)		observation time (s), number of flights	number concentration (1/cm³ stp)		observation time (s), number of flights	NH/SH factor
	median	range		median	range		
Aitken particles (d_p > 14 nm)	107	85...143		296	179...488		2.8
ultrafine particles (5 nm > d_p > 14 nm)	10	5...17	283,	222	104...661	1213,	22.2
accumulation mode part. (d_p > 120 nm)	43	29...69	2	93	66...139	8	2.2
non-volatile particles (d_p > 10 nm)	27	23...32		82	53...111		3.0

3.5. WP5: Residual particle properties
Start date: 0
End date: 24
Lead contractor: 1

The size distribution of residual particles was already investigated within the first reporting period. Clearly, differences could be found when comparing the distributions observed in the two hemispheres. The Southern Hemisphere data was characterized by larger residual particles than in the NH. Generally, the number density of residual particles is controlled by particles smaller than 100nm in diameter, which is common to both data sets.

The second reporting period was devoted to further analysis of the data and to upload primary observations to the database, which is accessible through the INCA web page. As part of collaboration between DLR, SU and Institute of Hydrochemistry, Technical University Munich, Germany, the first set of filter samples collected by the CVI-payload was analysed.

Sixteen samples of the cloud residuals from 6 different flights were collected on 0.4 μm pore size polycarbonate Nuclepore filters during the SH campaign based in Punta Arenas, Chile. The samples were analysed using Scanning Electron Microscope (SEM) equipped with Energy Dispersive Analysis of X-rays (EDAX). The number of particles per sample analysed varied between 30 and 45. The instrumental set up was able to detect particles larger than approximately 200 nm. Particles larger than 2.5 μm were excluded from analysis. Based on the SEM analysis, cloud residuals were divided into 4 major groups: crustal origin, sea-salt, anthropogenic origin, and not determined. Their relative fractions are listed in Table 3.5.1.

Table 3.5.1: Summary of the abundance of the four major groups of cirrus cloud residuals from SH campaign based on the SEM single particle analysis.

Type	Crustal	ND	Sea-salt	Anthropogenic
Fraction (%)	53	43	3	1

The last category are the type particles that can be seen on the filter but are composed of a light element (atomic number less than Na), composed of the same elements as the substrate (C and O) or contain the same material as the coating used (Ag). Hence, these particles cannot chemically be separated from the background signal. Often this type of particle is referred to as the organic fraction. Here we term them ND (Not Determined). The crustal category can be further subdivided by the element that is most dominant, such as Al-rich, Si-rich, or Fe-rich. The last category is the larges and represents almost 80%. These iron particles often contain Si, Cr, Mn, and Ni as well. An example is presented in Figure 3.5.1.

Approximately half of the crustal particles and 15 % of the ND-particles contain detectable amounts of sulphur. Occasionally, the sulphur appears together with Na, Cl and Mg, which might be reminiscence from liquid cloud processes. Pure sea-salt particles (Na-Mg-S-Cl) and anthropogenic particles (V-Fe-Ni, chain aggregates) only make up ca 4% of the analysed particles.

Based on the particle morphology, about 15 % of the cloud residuals may be attributed to plant fragments or pollen. Measurements of particle light absorption indicate that a large part of this undetermined organic fraction may contain soot.

Figure 3.5.2 show the average amount of absorbing material as a function of residual number density. We recall from the first report that there was an excellent agreement between the different cloud probes and that the number of residuals also can be viewed as the crystal number density.

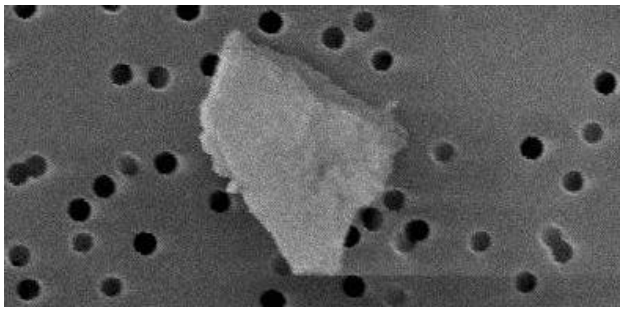

Figure 3.5.1 A crustal type particle present in cirrus crystal. Sample from Punta Arenas Campaign in Chile. The particle is approximately 2 μm across.

The similarity in the data from the two hemispheres presented in Figure 3.5.2 indicate that approximately the same amount of absorbing particles (by mass) are included in the crystals regardless of the observation is made in the SH or NH.

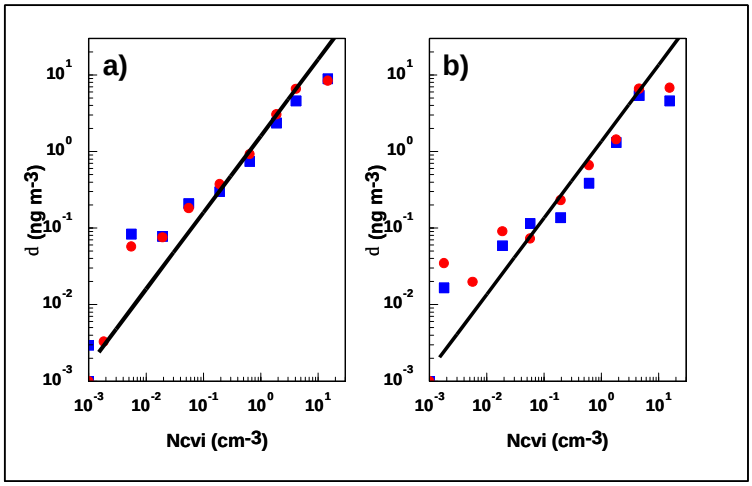

Figure 3.5.2 Mass concentration of absorbing particles incorporated into ice crystals as a function of the crystal number density, a) Punta Arenas and b) Prestwick. Blue squares and red dots are median and average values, respectively.

Although, there are very few reported measurements of ambient soot concentrations in the tropopause region, the few that do exists suggest that our observations are almost an order of magnitude higher. This is if one assumes that cirrus clouds can scavenge all the available soot. If only a fraction of the ambient soot is included in the crystals, the ambient concentrations of absorbing particles must be much larger than previously thought. The presence of pollen and large soot chains found in the filter samples and the increase in CO with altitude (see WP 6 on trace gases) suggests that the tropopause region in the SH mid-latitudes may be significantly affected by long-range transport.

Because many parameters are of importance for the formation and development of cirrus clouds it was necessary to illustrate the data in ways that reduced the influence from one or more parameters. One such plot is presented in Figure 3.5.3a.

Here simply the number of observations is shown in colour coding as function of relative humidity over ice (RHi) and the residual number density (Ncvi). Although, the range in number density extends over several orders of magnitude, there clearly exists a maximum at around 3 cm^{-3} and 100% RHi. Next we proceed by normalizing the number of observations to the maximum found for a given relative humidity. A very different plot appears and is presented in Figure 3.5.3b. The interpretation of this type of plot is that if different combination of Ncvi and RHi are related in time a pattern in the colour plot should appear. If not, the colour pattern would look like random mosaic. As can be seen in the Figure 3.5.3b there is a symmetry around 100% RHi and a branch at high RHI extending towards high Ncvi. The fact that a pattern can be seen in this type of plot suggests that this is a signature of the most preferred pathway for the evolution of the cloud in terms of Ncvi and RHi. Cirrus begins with high humidity and low number density. The crystals number density increase quickly in the beginning of the clouds life cycle. At first this occurs without any significant change in humidity. At some point the sink of water vapour by the crystals is larger than the supply and the relative humidity start to decrees. This part of the life cycle constitutes the growth regime of the cloud. As the humidity decrease below 100% the cloud particles begin to evaporate. This causes a decrease in the number of crystals as the humidity decrease.

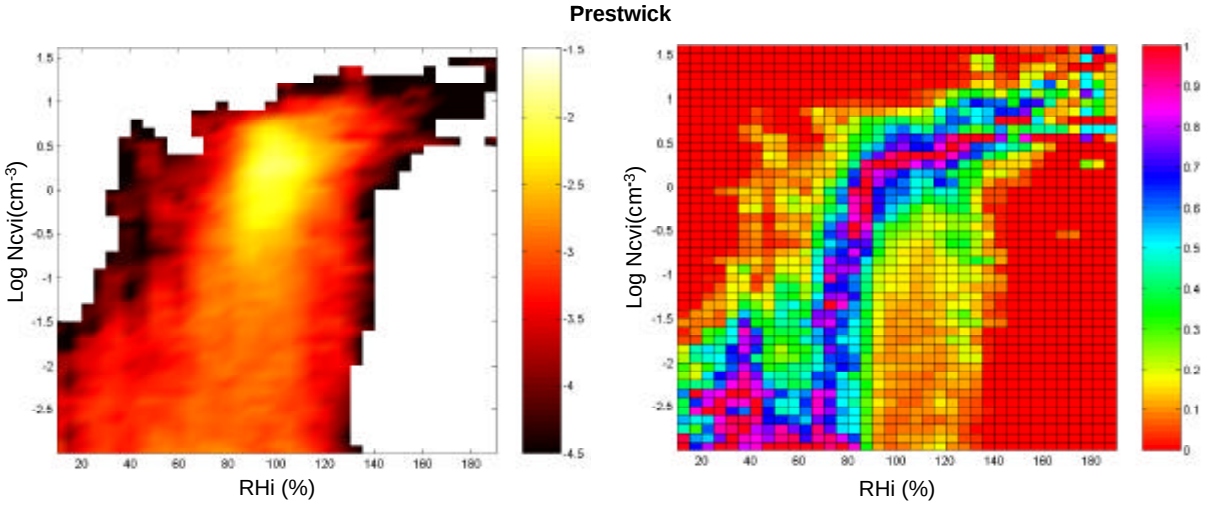

Figure 3.5.3 The frequency and normalized frequency of occurrence as function of relative humidity and crystal number density. The colour coding represents number of observations (a), and the number of observations normalized to the maximum value at each humidity bin (b). Hence, along a given humidity there is always a cell of the value of one. Data sampled at temperatures below 235K.

The scenario discussed above holds many similarities with the evolution found in a wave clouds. Indeed analysis shows that in average the vertical wind is positive at RHi above 100% and negative below. The results shown in Figures 3.5.3 a and b are very similar for the Punta Arenas campaign. Hence, a particular combination of RHi and Ncvi in affect represents a stage in the evolution of the cloud. We keep this in-sight when we proceed by plotting the fraction of non-volatile particles in the same format as above.

The distinction in volatile, semi-volatile and non-volatile particles is performed through the thermal stability of the particles. The sample air from the CVI is divided into three separate branches. The air is heated to three different temperatures 25, 125, and 250ºC. If a residual particle disappears after being heated to 125ºC it is

termed volatile. If it remains after heating to 250ºC it is termed non-volatile. Particles remaining in between these temperatures are termed semi-volatile. The fraction of non-volatile particles in the NH and SH are presented in Figure 3.5.4.

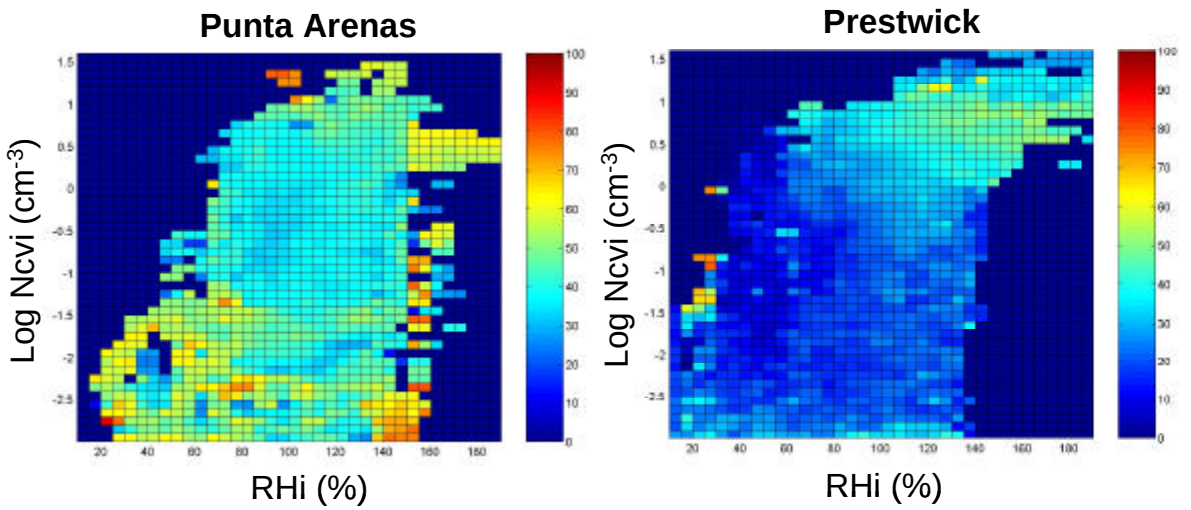

Figure 3.5.4 The fraction of non-soluble residual particles as function of relative humidity and crystal number density. The colour scale is in percent.

Two observations are made immediately. First, both data sets show an unexpected high fraction of no-volatile particles at temperatures below 235K. Second, this fraction is significantly larger in the southern hemisphere than in the northern hemisphere. The fraction of semi-volatile particles was very small and the fraction of volatile particles is essentially the complement to non-volatile particles. These are presented in figure 3.5.5. With increasing Ncvi and increasing Rhi the fracion of non-volatile particles increase. The reason for this is not clear, but it is possible that when high humidities are achieved in the cloud even particles consisting of a mixture of soluble and non-soluble material become activated and eventually become ice crystals.

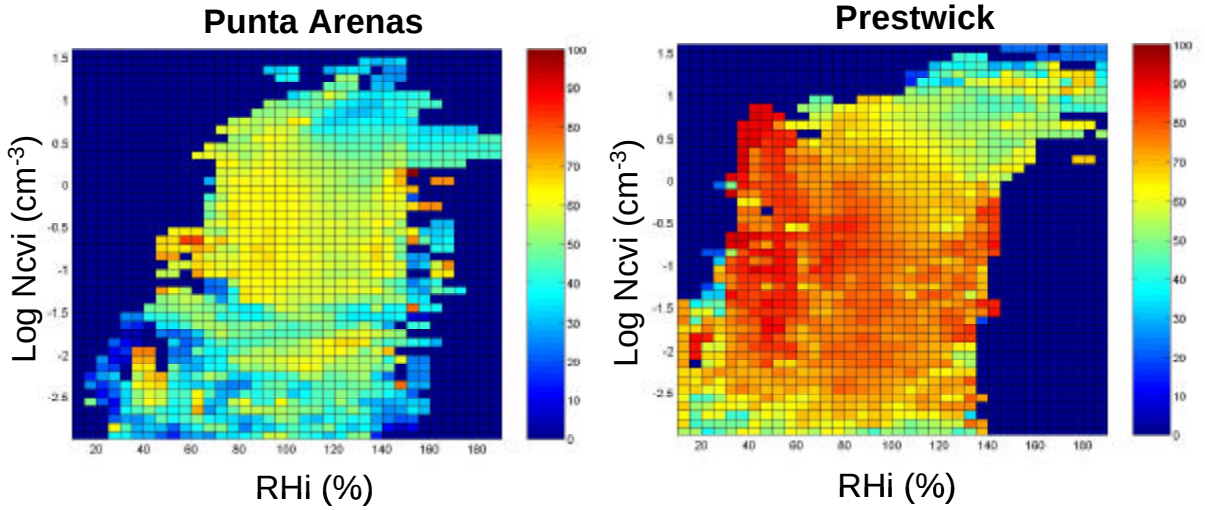

Figure 3.5.5 Same as 3.5.4 but for the volatile fraction.

The results presented above are the first of its kind and have generated new in-sight to the aerosol particles that participate in cirrus formation. The modes of ice nucleation is clearly not a strait forward problem.

3.6 WP6: Air mass Trace gases

Start date: 0
End date: 24
Lead contractor: 4

In situ observations of trace gas concentrations were performed with a set of instruments onboard the Falcon aircraft during the two campaigns, from Punta Arenas and Prestwick, during the first period of the contract. These instruments are Ozone, CO and NO/NOy analysers implemented by DLR, and a hygrometer implemented by LMD. During that second reporting period, the data obtained from the trace gas instruments for each Falcon flight have been analysed and put in the INCA database. Also are analysed and put in the data base, the data from the DLR instruments operated during the ferry flights between Oberpfafenhoffen and Punta Arenas, and between Oberpfafenhoffen and Prestwick.

Contribution from DLR

The data of the trace gas measurements (NO, NOx, NOy, CO, O_3) and the NO_2 – photolysis rate obtained during the two INCA campaigns and during the ferry flights have been provided to the INCA database.

The measurements performed during INCA contribute to the global trace gas climatology. Several aircraft campaigns were performed in the region of the North Atlantic flight corridor and in the Pacific region in recent years. However, trace gas measurements in remote regions of the southern hemisphere are sparse. The large data set acquired during the two INCA campaigns at local autumn at mid latitudes allows an interhemispheric comparison of NOx, NOy, O_3 and CO. The altitude profiles of these trace gases are shown in Figure 3.6.1.

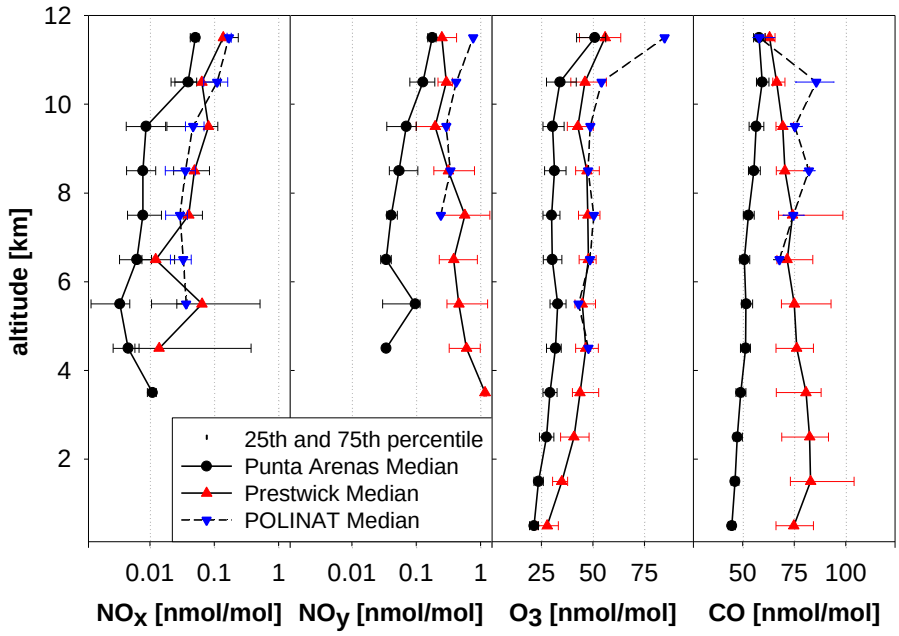

Figure 3.6.1: Altitude profiles of trace gases from INCA and POLINAT 2 campaigns. The amount of all the considered trace gases is clearly higher in NH than in SH. Also higher in NH is the variability of these amounts.

The significant difference in the trace gas loading of the troposphere in these two regimes reflects very well the expected higher source strength for these trace

species in the northern hemisphere. Also shown in Figure 3.6.1 are the altitude profiles obtained during the POLINAT 2 campaign in September and October 1997 in the region of the North Atlantic flight corridor (Shannon / Ireland). Overall, a good agreement was found between the INCA – Prestwick and the POLINAT 2 data set.

As mentioned above data suitable for comparison with the INCA – Punta Arenas data set are sparse. During STRATOZ III (Stratospheric Ozone Experiment) in June 1984 and TROPOZ II (Tropospheric Ozone Experiment) in January 1991 aircraft measurements were performed with a similar flight track between Europe and Chile as INCA. While the NOx measurements performed during STRATOZ III compare reasonable well with the INCA NOx profiles obtained in Punta Arenas, significantly higher NOx and NOy values were measured during TROPOZ II. A reasonable good agreement for CO and ozone was observed for all three campaigns.

The meridional trace gas distribution obtained during TROPOZ II was also compared with the values obtained during the southbound ferry flights of INCA. The TROPOZ II is better suited for comparison with INCA because both campaigns were performed during the South American wet season. It was found that in general the meridional distribution of NOx, NOy, CO and O_3 compare reasonable well.

The ozone production rate in the upper troposphere crucially depends on the background NOx concentration. Further analysis with the INCA data set will focus on the influence of the different trace gas levels observed at southern and northern mid latitudes on the oxidising capacity of the atmosphere.

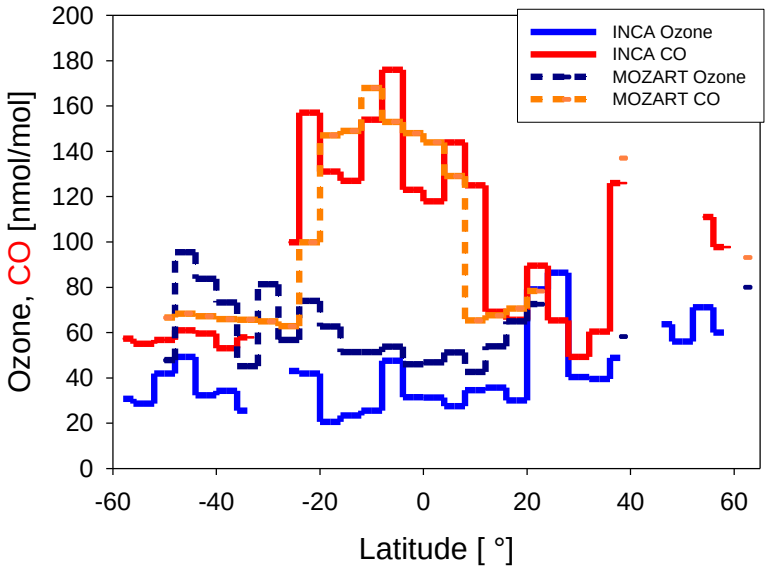

Figure 3.6.2 : Comparison between measurements during the ferry flight between Punta Arenas and Oberpfafenhoffen, and simulation from MOZART model.

Additionally, the results of the trace gas measurements performed during INCA were compared with model simulations. Collaboration started with Louisa Emmons from the NCAR – Atmospheric Chemistry Division in Boulder. In Figure 3.6.2, CO and ozone concentrations measured during the ferry flights between Oberpfaffenhofen and Punta Arenas in the upper troposphere are compared to results from the model simulations with the 3 – D chemistry transport model MOZART (Model for Ozone and Related chemical Tracers) of NCAR. The measured and simulated CO values agree very well. In general MOZART simulated higher ozone values than measured during INCA. Further model – measurement comparison as well as the analysis of the differences will be performed in the ongoing collaboration.

The analysis of the uptake of HNO_3 by cirrus cloud elements was continued. However, the complexity of the problem requires a very profound and time-consuming analysis. Particle NOy is calculated from the difference between forward and backward facing NOy sampling. The forward facing sampling requires the calculation of the enhancement factor that strongly depend on, among other parameters, the size dependent aerosol surface. Uncertainties do also arise from the unknown HNO_3 – fraction of total reactive nitrogen. A concluding statement concerning temperature and aerosol surface dependent NOy uptake is not yet possible. So far it was found that in general particle NOy amounts only a few pptv or a few percent of the available total NOy. Further analysis will also focus on possible interhemispheric differences of the NOy uptake. The possible mechanism of portioning of HNO_3 during nucleation is discussed in WP8.

Contribution from LMD

A large variety of meteorological conditions have been encountered during the flights for the two campaigns, as shown from the large range of ozone and water vapour mixing ratio in the air masses investigated.

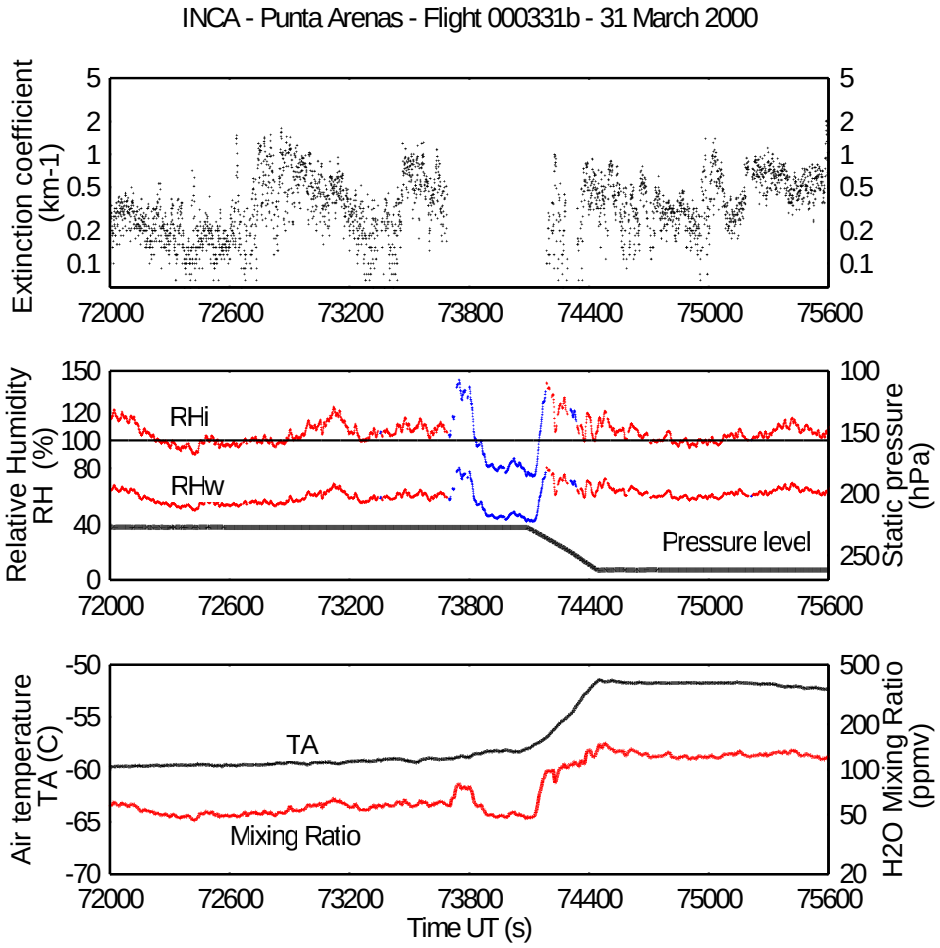

Figure 3.6.3. : Example of measurements from inside to outside cirrus cloud. The upper graph shows the extinction coefficient (WP3). The middle graph shows the Relative humidity with respect to liquid water (RHw) and with respect to ice (RHi), inside the cirrus red line, and outside blue line, following the extinction coefficient data. RHi is highly variable inside the cloud, above and around 100%, when at the edge of the cirrus the RHi is as high as 150%. The lower graph displays the temperature level and the H2O mixing ratio.

Water vapour, also being a trace gas, gives important insight into the behavior of cirrus clouds and its relation to the atmospheric composition. The observations were stratified into in-cloud and out-of-cloud cases. The criteria used was 0.05 km^{-1} threshold of the extinction coefficient measured by the Polar Nephelometer. Moreover, in order to be considered as in or out cloud data, the observed extinction coefficient must remain below or above the threshold for at least 4 consecutive seconds, to take into account the time response of the hygrometer. An example of an inside to outside cloud observation is displayed in Figure 3.6.3.

As most of the time the cirrus clouds are found to be ice supersaturated in both hemispheres, the histograms of the distribution of RHi for the two hemispheres has been carefully analysed, as displayed on Figure 3.6.4, using the distinction between in and out of clouds as explained before. It is seen that there is a higher frequency of RHi>100% in Southern Hemisphere (SH) than in Northern Hemisphere (NH), inside as well as outside cirrus clouds, though the maximum in the distribution is around RHi = 100% for the both set of data inside cirrus, that is to say at the level of ice particles equilibrium.

Outside cirrus, the distribution of data is related to the difference in cirrus coverage encountered during the two campaigns, as in the NH more time was spent in cloud free air, according to our criteria. In fact 42% of the analysed data are considered as “outside” cirrus clouds in SH compared to 59% in NH.

Inside cirrus clouds, the difference in the relative humidity repartition and supersaturation occurences has been related to the differences in the aerosol properties and quantities, as deduced from Work Package 4.

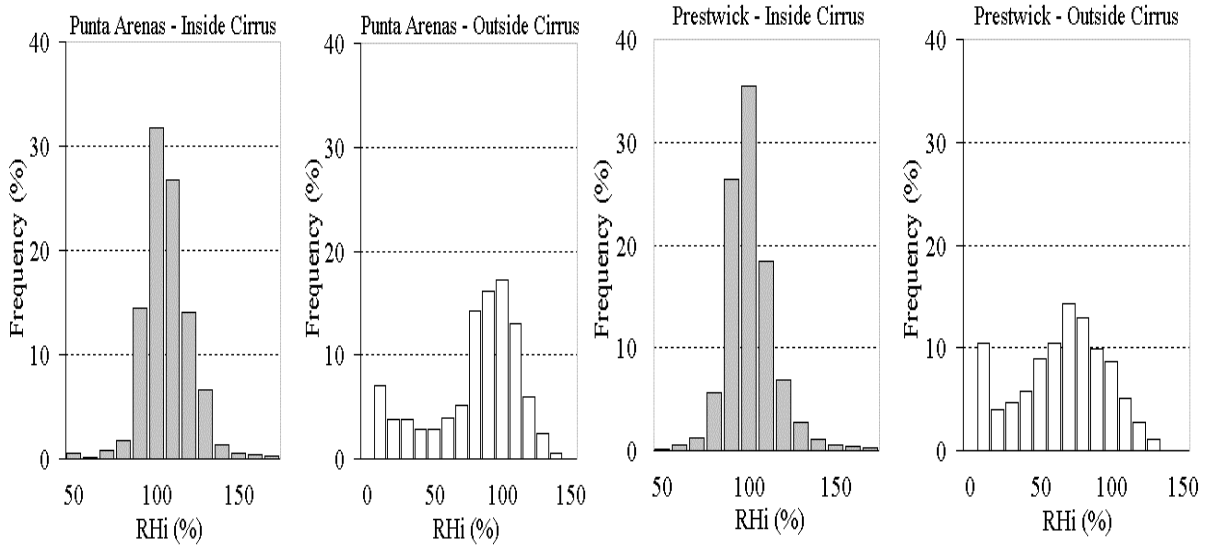

Figure 3.6.4 : Histograms of RHi measurement from Punta-Arenas and Prestwick, inside and outside cirrus clouds. Inside clouds there are 51% of the data with RHi >105% at Punta Arenas compared to 31% at Prestwick. For each location, the frequency is with respect to total number of data, inside and outside cirrus respectively.

3.7 WP7: Atmospheric State

Start date: 0
End date: 24
Lead contractor: 2

Atmospheric state data are basic parameters such as temperature, pressure, humidity, and wind, but crucial in the interpretation of all other observations and therefore stand as a task of its own. Especially, the extent of similarity or differences between the two campaigns is of special interest to the INCA project.

Contribution from DLR

All atmospheric state data measured during the mission flights are stored in an archive, which is accessible through the INCA homepage http://www.pa.op.dlr.de/inca/ . A first synopsis of these data shows some systematic interhemispheric differences. In Figure 3.7.1 vertical profiles for temperature, CO concentration and wind direction are shown for all mission flights. The temperature is slightly higher and more variable in Prestwick. The vertical distribution of the CO concentration is almost constant at a 40 to 50 ppbv level in Punta Arenas. In Prestwick there is a much higher variability, distinctly higher values at the ground, and some decrease of the concentration with altitude, which is indicative of a stratospheric influence. While the wind speed profiles are quite similar for both measuring sites, the wind direction shows obvious differences. In Punta Arenas the prevailing wind direction was West, in Prestwick the wind was blowing most of the time from either North or South. The stronger variability in the NH campaign is characteristic for most observed parameters.

Contribution from LMD

As the humidity is a primary parameter in cloud physics, in addition to the standard instruments of the Falcon, a frost point hygrometer associated to an air pressure sensor was operated by LMD to measure water vapour mixing ratio. Additionally, the relative humidity is determined by using the air temperature from the basic Falcon instrumentation, and a pressure correction is applied to retrieve the frost-point temperature of the outside, using the static pressure from the Falcon data. During the second period of the contract, the water vapour data have been carefully analysed, and data has been provided to the INCA data base for each flight, provided at 1 Hz sample rate, the water vapour mixing ratio, frost-point temperature, relative humidity with respect to liquid water (RHw), and the relative humidity with respect to ice (RHi).

As many occurrence of supersaturation with respect to ice were measured during both campaigns, the water vapour data have been analysed with a distinction between inside and outside cirrus clouds data. To perform that classification, the extinction coefficient from the polar nephelometer was used as explained in Work Package 6.

The figure 3.7.2 displays the repartition of the relative humidity for the two campaigns, inside and outside cirrus clouds, with respect to the air temperature.

Included in the panels of figure 3.7.2 are the liquid saturation level, and the homogeneous ice nucleation level using the relation derived from Koop et al (2000):

$$RHi = 338.7 - 0.398\ T \quad (RHi \text{ in } \%;\ T \text{ in } K)$$

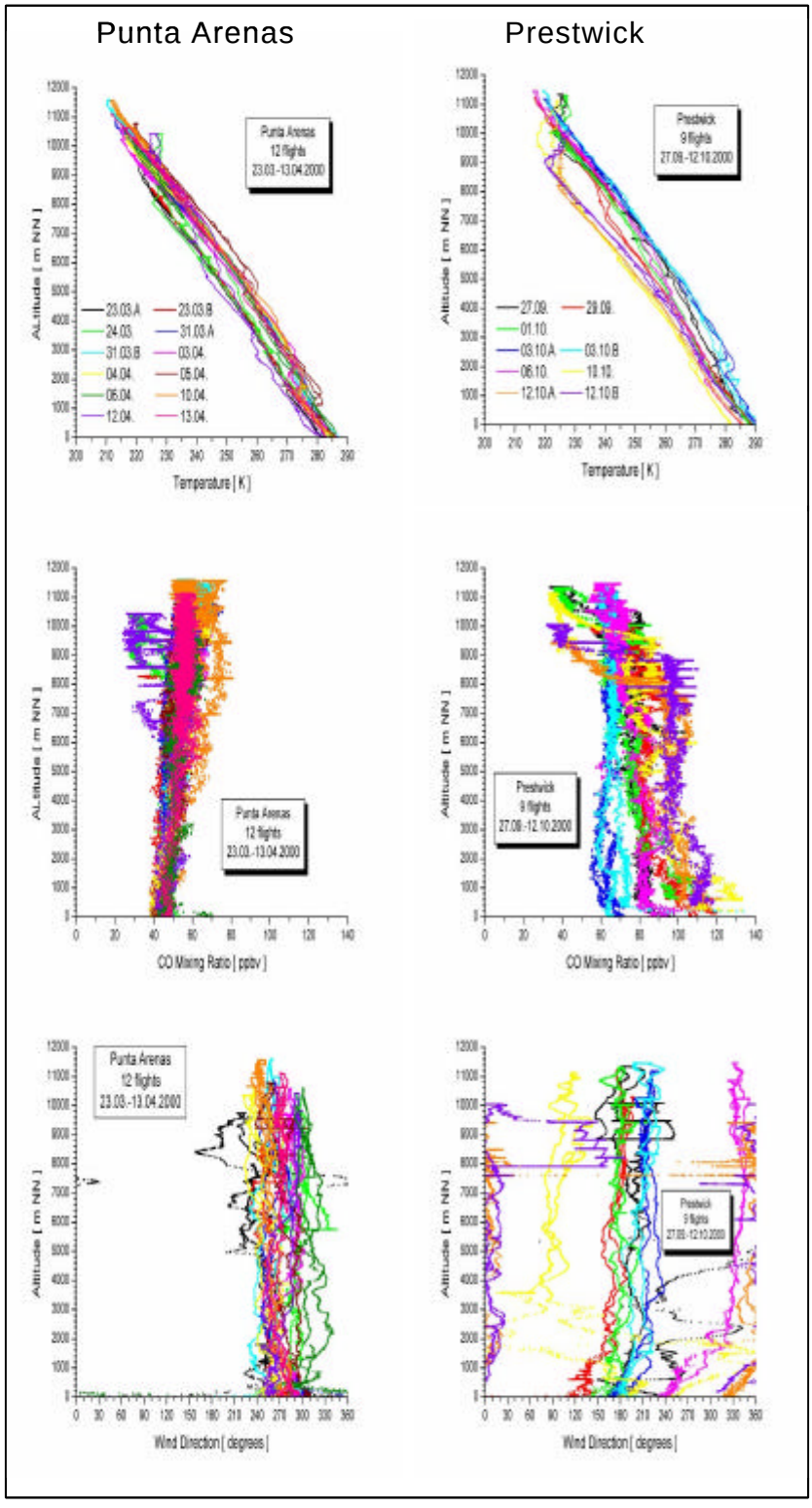

Figure 3.7.1. Vertical profiles of temperature, CO concentration, and wind direction for the mission flights in Punta Arenas (left) and Prestwick (right). The dates of the missions and the color code are shown in the temperature panel.

It is seen that, for both hemispheres, there are frequent occasions where the humidity exceed ice saturation and approach the homogeneous nucleation threshold inside as well as outside cirrus clouds. Sometimes RHi even exceeds water saturation at temperature below –40ºC. These events are very few and observed for

short time periods (few tens of seconds). These events are not supported by existing theories and artefacts cannot be excluded. However, the corresponding data have not been rejected from the data files in the database, as they are connected with strong signals in other observations. Moreover, as shown on figure 3.7.3 the standard instruments from the aircraft measure also large and sudden increase of water vapour content at the same time, as well as perturbations in the vertical wind velocity.

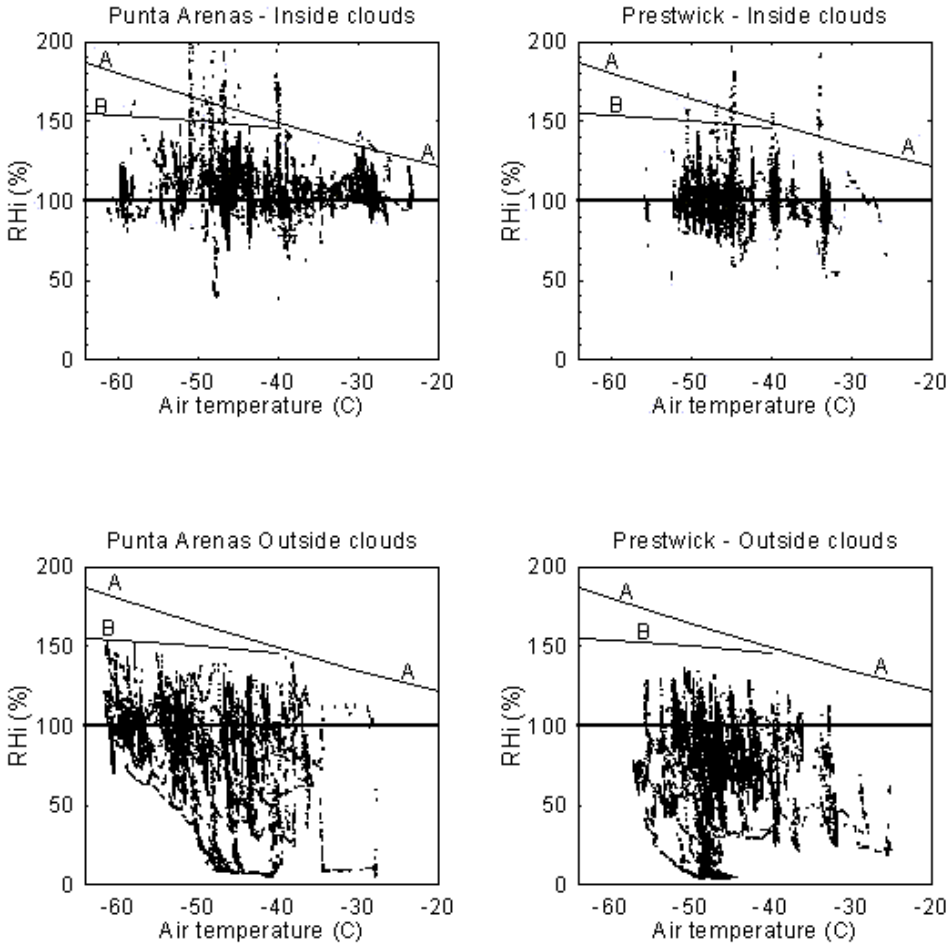

Figure 3.7.2.: Relation between the Relative humidity with respect to ice (RHi) and the air temperature, outside and inside cirrus clouds for both hemispheres. On each plate, the level for saturation with liquid water is displayed as line A, and the homogeneous ice nucleation level from Koop is displayed as line B (from Koop et al, Nature, 406, 611-614, 2000)

The data from the two campaigns was further analysed by generating histograms for the NH and SH, respectively. The resulting diagrams for conditions below –35ºC are presented in Figure 3.7.4. Above –40ºC the histograms are rather similar, but below –40ºC the two data sets begin to diverge. It is possible that this difference between the two campaigns is indicative of different formation thresholds for cirrus formation. The exact cause for this difference is not fully evaluated yet, but we note that also the atmospheric aerosol in the two hemispheres is different. The relative contribution below –40ºC of homogeneous and heterogeneous nucleation is a matter of controversies as the numerical modelling of the two processes is difficult and no direct observational evidence is currently available.

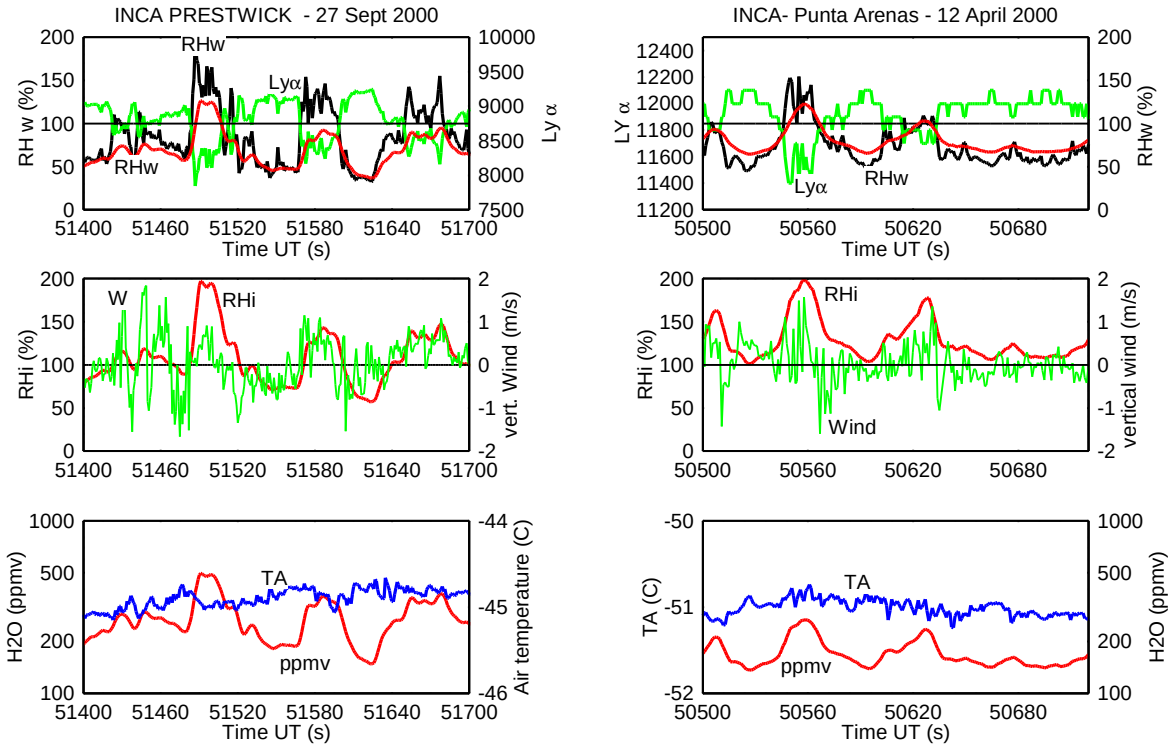

Figure 3.7.3. Examples of perturbations, when the relative humidity with respect to liquid water is estimated to be above 100% for short periods. On the upper graphs the black line is RHw from the Falcon, the green line is the output from the Falcon Lyman α hygrometer, and the red line is RHw from the frost-point hygrometer. As well, on the other graphs the red lines are data from frost point hygrometer. Perturbations in the vertical wind speed is displayed on the middle as green lines.

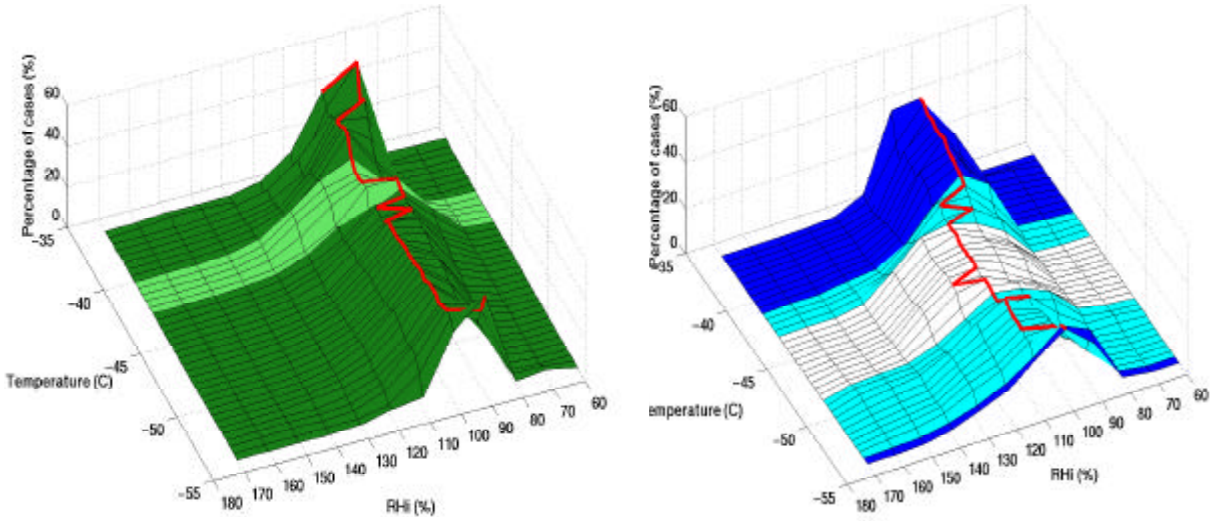

Figure 3.7.4. Histograms of RHi as function of temperature. The distribution becomes clearly dissymmetric towards large RHi below –40ºC in SH contrarily to NH where the distribution remains fairly symmetric with respect to 100% along the whole temperature range.

3.8 WP8: Process modelling
Start date: 13
End date: 24
Lead contractor: 5

We have used a mixed phase cloud model (MIXCLOUD) to estimate how much the measured gas phase HNO_3 is responsible for cirrus cloud particle growth, and whether the measured solid phase (cloud particle) HNO_3 concentrations can be explained by condensation of HNO_3 vapor onto initial cloud condensation nuclei (CCN) during cloud formation process

Initial values for MIXCLOUD model are adopted from INCA campaign experimental data, from which we have calculated minimum, average and maximum values. These values are calculated using data above 9 km height above sea level only, and thus calculated values are assumed to represent conditions in the upper troposphere in both NH and SH. Initial CN particles are assumed to be $H_2O/HNO_3/H_2SO_4$ solution droplets. In addition, nitric acid vapour and particulate concentrations are assumed to be equal to measured NO_y concentrations.

Table 8.1: Minimum, average and maximum INCA campaign NH and SH parameter value for some meteorological parameters and concentrations used in modeling. $[NO_y(p)]$ values presented in table are 1% of total measured $[NO_y(p)]$ values..

Parameter	Unit	NH			SH		
P_{stat}	mbar	197.12	261.78	320.91	195.83	239.53	338.39
T_{stat}	K	215.19	225.61	236.62	208.64	221.91	248.81
w_{up}	ms^{-1}	0.01	0.26	2.25	0.01	0.20	2.43
RH_{wat}	%	2.30	50.84	165.54	2.20	58.54	141.24
$[NO_y](g)$	pptv	61	525	4946	1	97	1343
$[NO_y](p)$	pptv	0.21	1.36	29.55	0.07	1.04	18.93

Model calculations were performed with the MIXCLOUD model. MIXCLOUD simulate an air parcel using detailed multicomponent condensation/evaporation model Kulmala *et al.,* 1993; Lehtinen *et al.*, 1998; Hienola *et al.*, 2001) and fully stochastic Poisson statistical freezing of liquid phase droplets. Initial aerosol is a mixture of gaseous water, nitric acid and sulphuric acid vapours, and multimodal log-normal distribution of aqueous droplets of these substances. Some fraction of initial aerosol particles can also be insoluble. Ice nucleation rate inside an aqueous droplet volume is calculated using a novel parameterisation by Koop *et al.* (2000). The model contains a stiff set of ordinary differential equations for air parcel temperature and total pressure, partial pressures of condensing species and mass fluxes of different condensing species for different size classes in liquid and solid phases. More detailed description of model is presented by Hienola *et al*. (2001).

The effect of particle size and chemical composition on particle activation is described by Kohler theory (see e.g. Laaksonen *et al*., 1998). According to this theory, the increase in particle size decreases the ambient saturation ratio that is needed for particle activation. Therefore, the larger particles activate at lower ambient saturation ratios in comparison with smaller particles which have the same chemical composition. Because of the continuous growth of activated particles, the water vapour is depleted from gas phase and at some point the ambient saturation ratio starts to decrease although the updraft motion of the air parcel continues. The growth of the activated particles prevent the activation of smaller particles, as the ambient saturation ratio decreases below the threshold for the smaller particles. As a

result, the smaller particles start to evaporate. This phenomenon is also known as Ostwald ripening.

At the beginning of simulation, air parcel starts to lift up with a constant updraft velocity. During the updraft motion, air parcel cools adiabatically, and saturation ratios of condensable vapours start to increase inducing condensational growth of initial $H_2O/HNO_3/H_2SO_4$ aerosol particles. If the initial aerosol in the model does not include solid phase particles, the freezing probability of aqueous phase droplets is calculated at every following time step in the MIXCLOUD model. If the probability of freezing is greater than zero for some size class, solid phase distribution is constructed and inserted into model, as described by Hienola *et al.*, (2001).

In our calculations, we use ice nucleation rate parameterisation described by Koop *et al*., 2000, which states that ice nucleation rate inside a volume of aqueous solution droplet depends only on water activity in solution and solution temperature. According to this parameterisation, the most diluted droplets tend to freeze before more concentrated ones. However, the largest interstitial droplets may not always be the most diluted ones, especially if the initial aerosol particles are iterated to equilibrium with their environment at initialisation stage of the model. The condensation of HNO_3 vapour onto particles can reduce water activity of smaller droplets more rapidly, in comparison with larger ones, although the absolute amount of condensing HNO_3 onto largest droplets is larger.

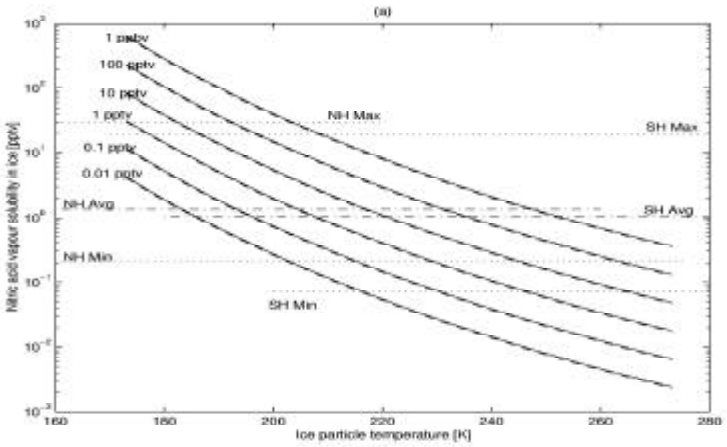

Figure 3.8.1. : Nitric acid solubility in ice [pptv] as a function of atmospheric temperature [K] and initial gas phase HNO_3 concentration [pptv] for typical NH (solid curves) and SH (dashed curves) atmospheric conditions. Different curves represent different initial nitric acid VMR values, which are marked next to curves. Horizontal lines represent minimum, average and maximum measured NH and SH concentrations of particulate nitric acid.

Therefore, HNO_3 enhanced condensation of water vapour on interstitial droplets tend to dilute smaller droplets faster than larger ones, due to larger surface area to volume fraction of smaller droplets (that is, smaller droplets can get into equilibrium with their environment faster than larger droplets). Owing to that, the time period how long liquid phase interstitial and activated droplets can grow before phase transition from liquid to solid becomes significant in removing water vapour from gas phase, has major effects on microphysical properties of resulting ice phase cloud. This in turn means that also the meteorological conditions such as air parcel updraft velocity (cooling rate), initial temperature and pressure, etc., can have significant effect on ice cloud formation process. E.g., if the air parcel initial temperature is high enough, there can be enough time for interstitial droplets to grow to cloud droplet sizes, before

freezing occurs. If initial temperature is relatively low, droplets can freeze already before they become activated, and the microphysical properties of resulting ice cloud can be totally different. Laboratory experiments by Dominé *et al.* (1996) suggest that in the given atmospheric temperature T [K] and partial pressure of nitric acid P_{HNO3} [hPa], the maximum solubility of nitric acid in ice $[HNO_3]_{max}$ [ppbm] is

$$[HNO_3]_{max} = 8.30\times10^{-12}\exp(3532.2/T)P_{HNO3}^{1/2.3} \qquad (3.8.1)$$

Using average NH and SH values for initial model parameters, we estimated the effect of condensable nitric acid vapor on cirrus cloud particle formation, with several different initial nitric acid volume mixing ratios varying from 1 pptv to 10 ppbv. These values cover approximately the range of values measured during INCA campaign. For air parcel constant updraft velocity, initial pressure and initial temperature we used the range of average values presented in Table 3.8.1

The effect of initial gas phase HNO_3 concentration on solid phase cloud particle number concentrations and geometric mean diameters (GMD) of activated solid phase cloud particle distributions are presented in Figure 3.8.1 and Table 8.3.1. Increasing gaseous phase HNO_3 volume mixing ratio clearly increases activated cloud particle number concentrations both in NH and SH cases (Fig. 8.1b). In NH case, the ice particle number concentration increase is about 74%, when gaseous phase nitric acid VMR is increased from 1 pptv to 10 ppbv. These values can be also thought as typical HNO_3 vapour concentrations in clean background and highly polluted air masses, respectively. In SH case, the increase is about 270%.

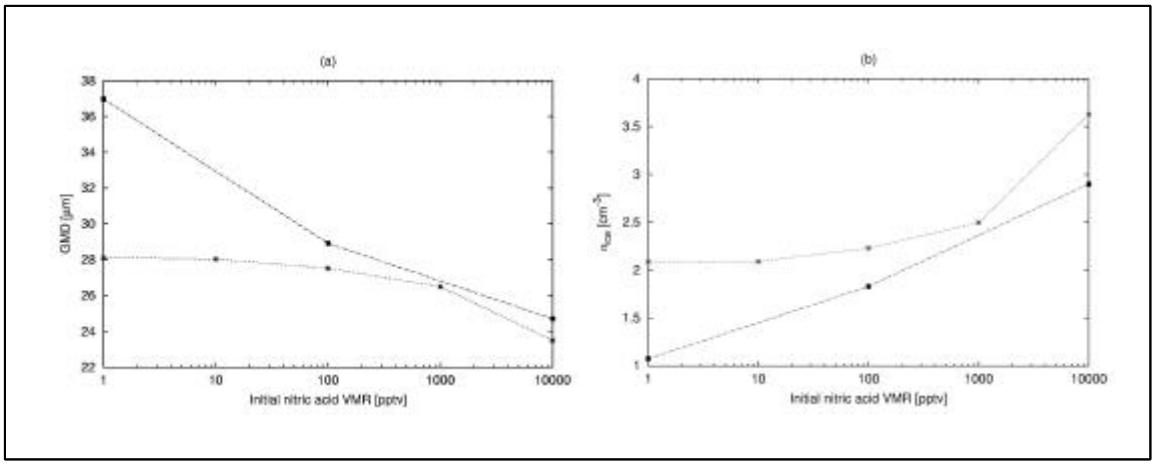

Figure 3.8.1. The effect of initial gas phase HNO_3 concentration increase on cirrus cloud microphysical properties (a) GMD [µm] and (b) number concentration n_{ice} [cm^{-3}] of solid phase cloud particle distribution in NH and SH as a function of initial HNO_3 vapour VMR [pptv].

Similar effect (but opposite relation) can be seen also in GMD of activated ice phase cloud particles (Fig. 8.1a). With increasing HNO_3 vapor VMR in gas phase, resulting ice phase cloud particle distributions GMD can decrease about 16% in NH case, and 33% in SH case, when nitric acid VMR is increased from 1 pptv to 10 ppbv, respectively.

In Figure 4, with increasing initial nitric acid VMR from background levels, the increase is stronger in SH case than in NH case with low nitric acid VMRs. In NH case, increase in number of cloud particles is strongest after about 1 ppbv value of initial nitric acid VMR. The aerosol loading in the NH is higher than in the SH, hence

the initial nitric acid concentration is divided between more particles, and the absolute amount of nitric acid in interstitial particles is somewhat smaller in NH case

Table 8.2. Modeled ice phase cloud particle distribution GMD [μm] and ice particle number concentration n_{ice} [cm^{-3}] as a function of initial gas phase nitric acid VMR $[HNO_3(g)]_0$ [pptv] for both NH and SH cases. Values presented in parenthesis are changes in percentages in comparison with our background case where nitric acid VMR $[HNO_3(g)]_0$ is 1 pptv.

$[HNO_3(g)]_0$	NH		SH	
[pptv]	GMD [μm]	n_{ice} [cm^{-3}]	GMD [μm]	n_{ice} [cm^{-3}]
1	28.096	2.0885	36.964	1.0748
10	28.034 (-0.2%)	2.0909 (+1.1%)	-	-
100	27.512 (-2.1)	2.2311 (+6.8%)	28.9120 (-21.8%)	1.8297 (+70.2%)
1000	26.494 (-5.7%)	2.4971 (+19.6%)	-	-
10000	23.482 (-16.4%)	3.6279 (+73.7%)	24.702 (-33.2%)	2.9011 (+269.9%)

Since nitric acid is a hygroscopic substance, an increase in gaseous phase nitric acid concentration also increases the amount of condensed phase nitric acid. At equilibrium, for all clouds of atmospheric interest, nitric acid is completely dissolved into cloud water, and its gas phase concentration is practically zero inside a cloud.

We have estimated the relative and absolute amounts of nitric acid substance condensed into particulate phase in atmospheric conditions during INCA NH and SH campaigns as a function of measured nitric acid gas phase volume mixing ratio. Mass fraction of condensed nitric acid is smaller in solid phase than in liquid phase, since only a fraction of the droplets freeze and become cirrus crystals. Moreover, the low nitric acid solubility in ice, described by Eq. (2), limits nitric acid uptake by ice particles

In Figures. 3.8.2a and b we have presented the total amount of condensed nitric acid in liquid and solid phase as parts per billion. Horizontal dotted and dashed lines represent measured particulate phase NO_y minimum, average and maximum. Thus, the model results presented in Figure 3.8.2a and b represent maximum values of ice phase HNO_3 uptake. According to our model results, it seems that the measured NO_y(p) concentrations are in agreement with measured NO_y(g) concentration values, and the concentrations in particulate phase could be explained by the condensation. We have assumed that all of the measured NO_y(g) and NO_y(p) are HNO_3 in our model input and output values, although the real HNO_3 fraction of NO_y is somewhat smaller.

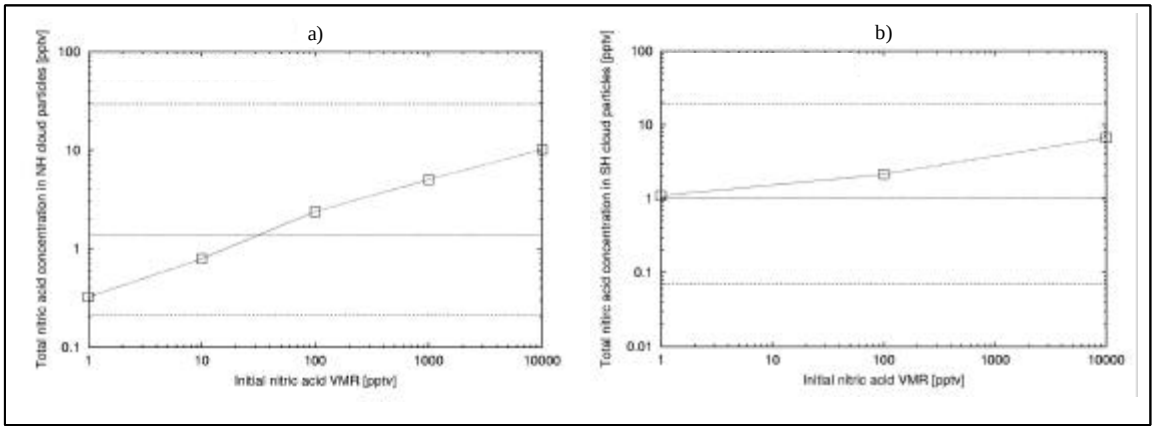

Figure 3.8.2 The effect of initial gas phase HNO_3 concentration increase on cirrus cloud particle HNO_3 uptake. Figs. (e) and (f) represent total condensed HNO_3 mixing ratio [ppbv] in NH (e) and SH (f) as a function of initial gas phase HNO_3 [pptv]. Dotted horizontal lines represent minimum, average and maximum values detected during INCA campaig.

4. Socio-economic relevance and policy implication

Many of the parameters measured in-situ as part of the INCA project revealed systematic differences between the two campaigns conducted in the Northern and Southern hemisphere mid-latitudes. For instance: number densities of aerosol particles where higher in the NH, number densities of ice crystals were higher in the NH, mean crystal sizes were larger in the SH, residual particles where larger in the SH, humidities where higher in the SH, and CO, O_3, and NOy where higher in the NH. All of these differences are most likely an effect of differences in the atmospheric composition due to the different pollution levels in the two hemispheres. For the mid-latitudes of the SH tropopause region there were until now no observational data available to confirm and quantify this large scale difference in parameters observed as part of INCA.

Changes in atmospheric composition caused by anthropogenic emissions are known to influence our environment in a detrimental way and acid rain and the ozone hole are outstanding examples of this. It is believed that changes in the air composition also influence cirrus clouds, especially their evolution as well as their microphysical properties. Changes in cirrus properties may in turn affect the radiation budget and climate, as well as air chemistry through heterogeneous reactions.

The work performed as part of the INCA project is therefore relevant with regards to the recent climate assessments (IPCC, WMO, EU) about the effect on cirrus clouds properties by anthropogenic emissions from sources at the Earth surface or from air traffic. For instance, the IPCC-Aviation report of 1999 states that the key uncertainty which has to be overcome in the future for better assessing the climate impact from aviation is the knowledge of contrail and aerosol impact on cirrus cloudiness. The even more recent report by the commission (chapter 7 of the Second assessment on stratospheric research) also emphasis this lack of understanding regarding the aviation impact on the atmosphere.

The INCA project help to fill some of the gaps and provide necessary knowledge to better assess current and future effects from anthropogenic emissions. It is these assessments that are used by policy makers to make long-term decisions that affect a large number of people. Hence, it is imperative that the best and most relevant information is available to make the best decisions and to find optimal solutions for environmental protection and a sustainable development.

The results obtained from the INCA project thus far, indicate differences in cirrus clouds that most likely are a result of different pollution levels in the two hemispheres. However, it is difficult to assess the sensitivity of the system. That is, how much can the environment be perturbed before a significant impact is observed? Clearly, the system is non-linear and one response to a perturbation may temporarily be masked by a counteracting response. This is analogous to the interplay between cooling of the climate by sulphate particles and the warming of the climate by carbon dioxide.

5. Discussion and conclusion

The trace gas levels of NO, NOy, NOx O_3, CO, observed at Prestwick significantly exceed the concentrations found at Punta Arenas indicating the higher pollution level at northern mid latitudes. The uptake of nitric acid by cloud elements is for the moment unclear, but it was found that only a few percent of the available gas phase NOy is incorporated into cirrus cloud elements. Weather this uptake arrives from deposition on the ice particle or originates as part of the nucleation process is still open. However, model simulations indicate that an enhanced level of HNO_3 in the ambient air could cause an increase in the crystal number density.

Aerosol levels are different in the two hemispheres, where the Northern Hemisphere show several times higher levels. To a large extent this is attributed to the different source strength of aerosol precursors in the two hemispheres. The different distribution of land and sea also play a role, since the large fraction of continents generates more convective transport of pollutants from the boundary layer.

The frequency distributions of relative humidity over ice show a shift in the mode towards higher values in the SH. The ambient conditions (temperature, vertical wind pressure distributions) in which the data was collected are very similar. It is conceivable that the difference in the humidity distributions is a result in the different aerosol loading of the two hemispheres. Exact how this works is not fully clear.

The data obtained for residual particles clearly show that both the size and the composition of the residual particles are different in the two hemispheres. The particle incorporated into the cirrus crystals are in average larger and contain a larger fraction of non-volatile particles in the SH. If this is a cause or effect of the different relative humidities observed in the two hemispheres is still a matter to resolve.

After normalizing the data to same relative humidity the observations show a systematic difference in the microphysical properties between the hemispheres. The crystals in the NH are more numerous and are smaller than in the SH for the same relative humidity. This is despite the fact that the cloud water content is higher in the NH for the same humidity.

An important fact, manifested by INCA data, is the ubiquitous presence of small crystals in cirrus clouds. This has already been reported in some previous studies, but never with so many independent observation techniques operational at the same time. The use of FSSP-300, PMS-2DC, Polar Nephelometer, and the CVI probe all converge to the fact that small crystals are important in characterizing a cirrus cloud.

The initial number density of ice crystals formed in cirrus is hypothesized to be determined by the peak in relative humidity and depends strongly on the updraft velocity and on temperature (Kärcher and Lohmann, 2001). Comparing our two data sets performed on a very similar temperature range and considering the relative humidity as an independent parameter, our observations suggest that differences in nucleation processes (and aerosol composition) must also be considered in order to explain the differences in the microphysical properties in the observed cirrus clouds. This is further supported by the differences in the observed aerosol properties.

Gierens et al. (2000) discussed a possible difference in the formation of cirrus in the two hemispheres based on a comparison correlation between sub-visible cirrus observed by SAGE II and the fractional cover of cirrus from EMCWF. Based on this comparison the authors suggest that cirrus formation in the Southern Hemisphere would be controlled more by thermodynamics, whereas in Northern Hemisphere freezing properties of the aerosol would dominate the cirrus formation.

Although much remain to investigate using the wealth of data produced within in the INCA project, we can conclude that the project accomplished what it sat out to do and the objectives are met.

- **The first observations of aerosols and cirrus properties in the Southern Hemisphere mid-latitudes have been collected.**

- **Observations of aerosol and cirrus properties in air masses of very different aerosol loading have been collected.**

These data have given new in-sight about the possible relation between anthropogenic emissions and cirrus properties that are of importance for assessing the role of human activities for changes of the climate and in the ozone distribution.

5 Plan and objectives for the future

The INCA project is terminated but many ideas to exploit the data further exists and the work with the data also spawn new questions. Below we list a number of ongoing and planed activities related to the use of INCA data.

- Insights on formation and evolution of cirrus clouds in SH versus NH might be derived from the analysis on the dependence of cirrus clouds on air mass properties (in terms of aerosol characteristics and humidity).

- Implementation of the inversion technique to retrieve the microphysical parameters in ice clouds (ice particle concentration, effective diameter, etc.) by using measured scattering phase function.

- Validation of retrieval techniques of microphysical and optical cirrus properties from satellite instruments (Terra MODIS, GEOS, AVHRR, ATSR). Coordinated measurements in space and time are available from both in situ and satellite measurements.

- Validation of retrieval techniques of microphysical and optical cirrus properties from Lidar measurements. Specific flight patterns carried out over the AWI lidar will serve to make comparison and interpretation of active remote measurements of cirrus properties.

- Implementation of upcoming numerical simulations. The in situ and remote sensing observations will serve as a basis for upcoming numerical simulations to help interpreting the results and data from the experiments.

- The data analyses and results of interpretation will be published in reports and scientific journals.

- First analysis of how representative the INCA data is in terms of season and region indicate that no extreme year where encountered in any of the campaigns. However, a more extensive analysis is required to show this in all aspects of the data. This is of importance for making generalisations of the results.

- The aerosol-cloud interaction works both ways and a deeper analysis on how clouds also may affect the aerosol through scavenging or even enhance particle production is currently on the way.

- The phase partition of chemical species will be completed once all the filter analysis are completed. Both interstitial and cloud residual samples were collected within the two campaigns.

- During INCA measurements were also conducted during the ferry flights. The amount of flight hours required was in the same order of magnitudes as the field campaigns. Several interesting features were observed (e.g. clouds in the stratosphere, anvil outflow in the tropics, the crossing of the ITCZ). These observations are also to be analysed.

The results of the INCA campaigns are also used for planning further related experiments. Presently experimental investigations on cirrus clouds are performed in the course of the project PAZI (http://www.pa.op.dlr.de/¨pazi/) and by cooperating in the NERC funded projects EMERALD 1 and 2. Details can be found on the following web pages:

http://users.aber.ac.uk/ccc97/emerald.htm
http://www.aber.ac.uk/~dphwww/staff/jjw.shtml
http://users.aber.ac.uk/ccc97/emerald/equipment.htm

7 References

Dominé, F., E. Thibert, et al., Interactions of gas-phase HCl and HNO_3 with ice, Chemical exchange between the atmosphere and polar snow, E. W. a. R. Bales, New-York, Springer-Verlag, 43, 1996.

Hienola, J., M. Kulmala, and A. Laaksonen, Condensation and evaporation of water vapor in mixed aerosols of liquid droplets and ice: numerical comparison of growth rate expressions, *J. Aerosol Sci.*, *32* , 351–374, 2001.

Koop, T., B. Luo, A. Tsias, and T. Peter, Water activity as the determinant for homogenous ice nucleation in aqueous solutions, *Nature*, *406*, 611–614, 2000.

Kulmala, M., A. Laaksonen, P. Korhonen, T. Vesala, T. Ahonen, and J. C. Barrett, The effect of atmospheric nitric acid vapor on cloud condensation, *J. Geophys. Res.*, *98*, 22949–22958, 1993.

Kristensson A., J-F Gayet; J. Ström, F. Auriol, 2000: In situ observations of a reduction in effective crystal diameter in cirrus clouds near flight corridors, *Geophys. Res. Lett*., 27, 681-684

Laaksonen, A., P. Korhonen, M. Kulmala, and R. Charlson, Modification of the Köhler equation to include soluble trace gases and slightly soluble substance, *J. Atmos. Sci.*, *55*, 853–862, 1998.

Lehtinen, K. E. J., M. Kulmala, T. Vesala, and J. K. Jokiniemi, Analytical methods to calculate condensation rates of a multicomponent droplet, *J. Aerosol Sci.*, *29*, 1035–1044, 1998.

Gierens K., U. Schumann, M. Helten, H. Smit and A. Marenco, A distribution law for relative humidity in the upper troposphere and lower stratosphere derived from three years of MOZAIC measurements, *Ann. Geophys.,* 17, 1218-1226, 1999.

Gierens, K., M. Monier, and J.–F. Gayet, The deposition coefficient and its role for cirrus clouds. Geophys. Res. Lett. (in press).

Gayet Jean–François, Frédérique Auriol, Andreas Minikin, Johan Ström, Marco Seifert, Radovan Krejci, Andreas Petzold, Guy Febvre and Ulrich Schumann. Quantitative measurement of the microphysical and optical properties of cirrus clouds with four different in situ probes: Evidence of small ice crystals Geophys. Res. Lett (in press).

Koop, T., B. Luo, A. Tsias, and T. Peter, 2000: Water activity as the determinant for homogenous ice nucleation in aqueous solutions, *Nature*, *406*, 611–614,

Kärcher,B. and U. Lohmann, 2001: Parameterization of Cirrus Cloud Formation. 2001, J. Geophys. Res.

Ström, J, and S. Ohlsson, 1998: In situ measurements of enhanced crystal number densities in cirrus clouds caused by aircraft exhaust. J. Geophys. Res., 103, 11355-11361.

8 Acknowledgements

The INCA team acknowledge the fruitful collaboration with the associated partners that became a great complement to the original project

Thanks to secretaries, assistants, workshops, flight crews, airport staff, students, scientists, PI's, families and who ever else made that little or big extra for the success of the INCA project.

Thanks to funding agencies; the European Commission, national agenesis, and the institutes and universities of the partners and associated partners.